## ORIGINAL RESEARCH

Human-Derived *Bifidobacterium dentium* Modulates the Mammalian Serotonergic System and Gut–Brain Axis

Melinda A. Engevik,[1,2,*] Berkley Luck,[1,2,*] Chonnikant Visuthranukul,[1,2,3] Faith D. Ihekweazu,[4] Amy C. Engevik,[5] Zhongcheng Shi,[1,2] Heather A. Danhof,[6] Alexandra L. Chang-Graham,[6] Anne Hall,[1,2,6] Bradley T. Endres,[7] Sigmund J. Haidacher,[1,2] Thomas D. Horvath,[1,2] Anthony M. Haag,[1,2] Sridevi Devaraj,[1,2] Kevin W. Garey,[7] Robert A. Britton,[6] Joseph M. Hyser,[6] Noah F. Shroyer,[8] and James Versalovic[1,2]

[1]Department of Pathology and Immunology, Baylor College of Medicine, Houston, Texas; [4]Pediatric Gastroenterology, Hepatology and Nutrition, Texas Children's Hospital, Baylor College of Medicine, Houston, Texas; [6]Department of Virology and Microbiology, Baylor College of Medicine, Houston, Texas; [8]Section of Gastroenterology and Hepatology, Department of Medicine, Baylor College of Medicine, Houston, Texas; [2]Department of Pathology, Texas Children's Hospital, Houston, Texas; [3]Department of Pediatrics, Pediatric Nutrition Special Task Force for Activating Research (STAR), Faculty of Medicine, Chulalongkorn University, Bangkok, Thailand; [5]Department of Surgical Sciences, Vanderbilt University Medical Center, Nashville Tennessee; and [7]Department of Pharmacy Practice and Translational Research, University of Houston College of Pharmacy, Houston, Texas
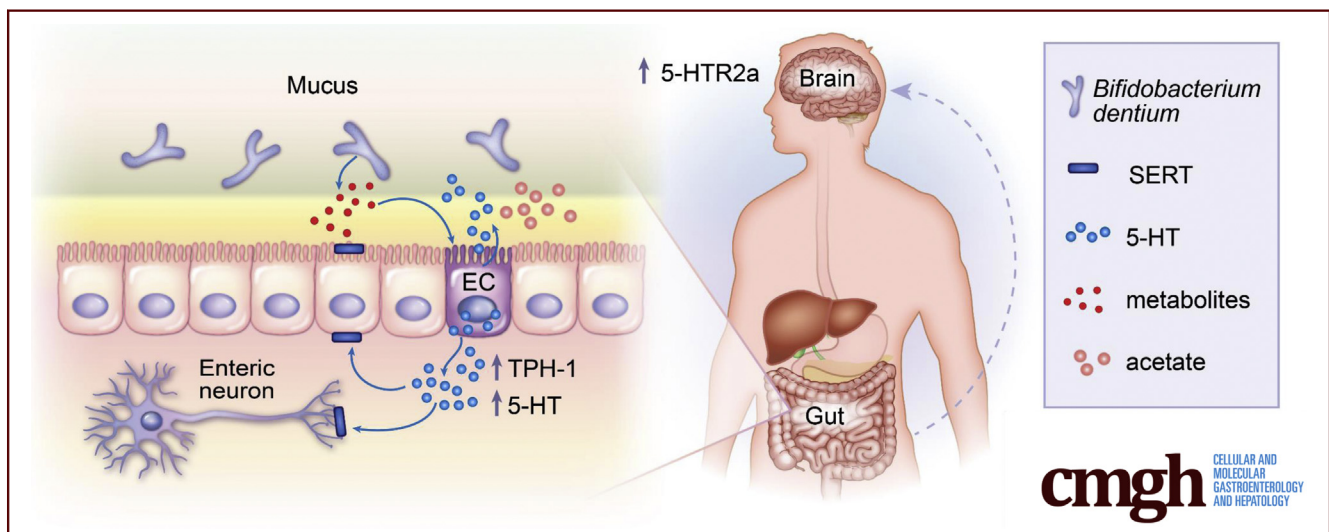
SUMMARY

By using gnotobiotic mice, and mouse and human intestinal enteroids, we found that *Bifidobacterium dentium*–produced acetate stimulates 5-hydroxytryptamine production from enterochromaffin cells. In addition, we show that *B dentium* modulates 5-hydroxytryptamine–receptor expression in the gut and brain and modifies behavior.

BACKGROUND & AIMS: The human gut microbiota can regulate production of serotonin (5-hydroxytryptamine [5-HT]) from enterochromaffin cells. However, the mechanisms underlying microbial-induced serotonin signaling are not well understood.

METHODS: Adult germ-free mice were treated with sterile media, live *Bifidobacterium dentium*, heat-killed *B dentium,* or live

Bacteroides ovatus. Mouse and human enteroids were used to assess the effects of *B dentium* metabolites on 5-HT release from enterochromaffin cells. In vitro and in vivo short-chain fatty acids and 5-HT levels were assessed by mass spectrometry. Expression of tryptophan hydroxylase, short-chain fatty acid receptor free fatty acid receptor 2, 5-HT receptors, and the 5-HT re-uptake transporter (serotonin transporter) were assessed by quantitative polymerase chain reaction and immunostaining. RNA in situ hybridization assessed 5-HT–receptor expression in the brain, and 5-HT–receptor–dependent behavior was evaluated using the marble burying test.

RESULTS: *B dentium* mono-associated mice showed increased fecal acetate. This finding corresponded with increased intestinal 5-HT concentrations and increased expression of 5-HT receptors 2a, 4, and serotonin transporter. These effects were absent in *B ovatus*-treated mice. Application of acetate and *B dentium*–secreted products stimulated 5-HT release in mouse

and human enteroids. In situ hybridization of brain tissue also showed significantly increased hippocampal expression of 5-HT–receptor 2a in *B dentium*–treated mice relative to germ-free controls. Functionally, *B dentium* colonization normalized species-typical repetitive and anxiety-like behaviors previously shown to be linked to 5-HT–receptor 2a.

CONCLUSIONS: These data suggest that *B dentium*, and the bacterial metabolite acetate, are capable of regulating key components of the serotonergic system in multiple host tissues, and are associated with a functional change in adult behavior. *(Cell Mol Gastroenterol Hepatol 2021;11:221–248; https://doi.org/10.1016/j.jcmgh.2020.08.002)*

The gastrointestinal (GI) tract supports a rich microbial community capable of modulating the host.[1–3] Recent work has identified an essential role for a complex microbiota in regulation of host-derived serotonin (5-hydroxytryptamine [5-HT]). Intestinal enterochromaffin cells synthesize the majority of the body's 5-HT via the enzyme tryptophan hydroxylase-1 (TTHP-1).[4–6] Enterochromaffin cell stimulation releases the stored 5-HT,[4,7–9] which can activate up to 14 different intestinal and neuronal 5-HT–receptor subtypes.[10–13] 5-HT can stimulate a number of targets in the GI tract, while also modulating the gut–brain axis to affect both anxiety-like and repetitive or impulsive behaviors.[14–16]

Evidence from studies using germ-free mice have suggested that a lack of gut microbiota causes impaired 5-HT signaling. In comparison with specific pathogen-free (SPF) mice with an intact microbiota, germ-free mice have altered 5-HT concentrations and turnover in the brain, decreased levels of circulating 5-HT and its precursor L-tryptophan, and decreased cecal and fecal 5-HT.[14,17–21] Germ-free mice also show aberrant behavior including reduced anxiety-like behaviors, diminished repetitive behaviors, and decreased cognitive function relative to mice with a complete gut microbiota.[22–24] Because 5-HT has been implicated in a variety of emotional, cognitive, and behavioral control processes,[14–16] the observed 5-HT deficiency in germ-free mice may help explain these behaviors. Together, the evidence suggests that a lack of a gut microbiota impacts 5-HT pathways and complex behaviors.

Studies have shown that gut microbiota modulate the GI serotonergic system; although the specific bacterial species and mechanisms of regulation remain unclear. Addition of human gut microbiota to germ-free mice increases *Tph-1* expression and colonic 5-HT concentrations.[25] Moreover, addition of spore-forming microbes from healthy mice and humans to germ-free mice promotes 5-HT biosynthesis by colonic enterochromaffin cells, resulting in increased serum 5-HT concentrations.[18] Human gut microbes do not appear to synthesize 5-HT,[17] indicating that bacterial stimulation of mammalian 5-HT secretion is pivotal in governing 5-HT biochemistry in the host. These previous studies[17,18,25]

provide strong evidence for microbial regulation of 5-HT. However, previously published work has described the effects of complex microbial communities, rather than defined bacterial species, in a gnotobiotic host. It remains to be elucidated which bacterial species stimulate 5-HT production, and the molecular pathways of microbial-induced serotonin signaling between the gut and central nervous system.

5-HT secretion is influenced by microbial-produced short-chain fatty acids (SCFAs), which are sensed by G-protein–coupled receptors 40 and 43, also known as free fatty acid receptor 2 and 3 (FFAR2 and FFAR3).[26–33] Acetate is the most abundant colonic SCFA and is known to preferentially signal through FFAR2.[26,34,35] Luminal stimulation of FFAR2 with the agonist phenylacetamide-1 in rat intestinal loops stimulates 5-HT release.[32,33] Moreover, exposure of mouse intestinal enteroids to acetate stimulates 5-HT release,[36] indicating a functional link between SCFAs and 5-HT. Commensal *Bifidobacterium* species include a number of acetate-producing taxa,[37–40] which have been shown to protect mice from a lethal infection with enterohemorrhagic *Escherichia coli* O157:H7[38,39] and is important for microbial cross-talk.[40] *Bifidobacterium dentium* is an acetate-producing colonizer of the healthy adult GI tract,[41] and has been reported to modulate sensory neuronal activity in a rat fecal retention model of visceral hypersensitivity.[42] Thus, we reasoned that *B dentium* would be an ideal choice to address the question of whether specific commensal bacteria alter in vivo acetate concentrations and modulate the serotonergic system in mammals.

In this study, we show that *B dentium*–produced metabolites stimulate 5-HT release from enterochromaffin cells both in vitro and in vivo. We observed that *B dentium*–colonized mice showed increased intestinal acetate and increased 5-HT concentrations in the intestinal lumen. These effects were not observed in mice treated with heat-killed *B dentium* or mono-associated with another commensal microbe: *Bacteroides ovatus*. *B dentium* mono-association also altered the expression of several key intestinal serotonin receptors, particularly isoforms 2a (*Htr2a*), and 4 (*Htr4*), and the 5-HT transporter, serotonin

Most current article

transporter (*Sert*), compared with germ-free controls. In addition, *B dentium*–colonized mice up-regulated expression of *Htr2a* in the hippocampus and colonization normalized the anxiolytic behavior observed in germ-free mice during the marble bury test. Together, these data show that *B dentium* can modulate serotonin-receptor–mediated signaling in the gut and brain of a gnotobiotic mammal.

Results

B dentium *Colonizes the Adult Germ-Free Mouse Intestine*

Adult Swiss Webster germ-free mice were divided into 2 groups, splitting mice from the same litters evenly. Both male and female mice were tested to account for possible sex-dependent effects. The mice were housed in separate isolators and were orally gavaged with *B dentium* on days 1, 3, 5, and 14 of the experiment to promote colonization. The *B dentium* treatment consisted of 2×10^8 viable *B dentium* cells in 200 μL MRS bacterial culture media, resulting in colonization of the mice after day 1 of treatment. As a control, germ-free mice were gavaged with 200 μL sterile MRS media or heat-killed *B dentium*. *B dentium* mono-association and verification of germ-free status was tracked via tissue staining, FISH, qPCR, conventional plating, and scanning electron microscopy (Figure 1). To assess the regions of *B dentium* colonization, sections of ileum and colon were examined by tissue Gram staining (Figure 1*A*). Compared with germ-free controls, *B dentium* mono-associated mice showed colonization of the mucus layer of the ileum, with increasing abundance observed in the colon. In contrast, only a few heat-killed *B dentium* were observable in the colon. This finding was confirmed further by FISH using a *Bifidobacterium* genus-specific probe (Bif164) in germ-free and live *B dentium* mono-associated mice colon (Figure 1*B*).

To confirm colonization, fresh fecal pellets were collected throughout the 2-week oral gavage period. Conventional agar plating and quantitative PCR analysis of genomic DNA extracted from feces confirmed *B dentium* colonization (Figure 1*C*). Approximately 1×10^8 CFU of *B dentium* was observed per gram of mouse feces (Figure 1*C*). No growth was observed in germ-free or heat-killed *B dentium*–treated mouse stool. To confirm that *B dentium* was able to adhere to intestinal cells, the human mucus-producing colonic cell line LS174T was incubated with *B dentium* for 1 hour, thoroughly washed, and then examined by scanning electron microscopy. *B dentium* was localized near the surface of these mucus-producing cells (Figure 1*D*). This finding correlated well with scanning electron microscopy analysis of tissue from *B dentium* mono-associated mice, where bacteria were found above the epithelium (Figure 1*E*). We also assessed the weight of the mice upon exiting the isolators (Figure 1*F*) and observed no significant differences between groups. In addition, we measured villus height in the ileum and crypt depth in the colons of germ-free and treated mice and also observed no differences (Figure 1*G* and *H*). Likewise, no changes were observed in the lengths of either the small or large intestine (data not shown). Taken together, these data show that *B dentium*

successfully colonizes the mouse intestine, but does not influence weight or intestinal morphology.

B dentium *Mono-associated Mice Have Increased Intestinal Acetate and 5-HT Concentrations*

Consistent with genome annotation and predicted functional SCFA output (KEGG map 01120; EC1.8.1.4),[72] *B dentium* was found to produce 1549.6 μM acetate in LDM4 in vitro. These findings were reflected in vivo as *B dentium* mono-associated mice showed significantly increased acetate concentrations in their feces compared with germ-free controls. No other significant differences were found among the other SCFAs tested (Figure 2*A*).

The intestinal epithelium is composed of a heterogenous collection of specialized cells that perform various functions in health and disease. One important cell type is the enterochromaffin cell, an enteroendocrine cell subtype, which has been shown to play a key role in serotonergic signaling.[4,20,73–75] Enterochromaffin cells contribute to intestinal homeostasis through sensing and responding to signals from the intestinal environment. One important component contributing to enterochromaffin cell responses to SCFAs is the G-protein–coupled receptor FFAR2.[27,28,30,32,33,76] We established that the FFAR2 receptor was expressed in select subsets of 5-HT–positive cells in our germ-free mice (Figure 2*B*), suggesting that SCFA-mediated processes, such as 5-HT release, may be occurring in vivo. Immunostaining showed no changes in ileal FFAR2 between germ-free, live, *B dentium*–treated, or heat-killed *B dentium*–treated mice (Figure 2*C* and *D*). However, we did observe increased colonic FFAR2 staining in enterocytes and enteroendocrine cells in live *B dentium*–treated mice compared with germ-free or heat-killed *B dentium*–treated controls. This increase in staining was reflected in the level of *Ffar2* mRNA in the colon (Figure 2*E*). These data suggest that FFAR2 may be able to mediate some *B dentium* signals in enteroendocrine cells.

We postulated that FFARs may stimulate 5-HT release in response to microbial-produced acetate. To address this question, we first determined that *B dentium* does not contain the gene pathway for the production of 5-HT (KEGG), and we confirmed that 5-HT was not detectable in bacterial media inoculated with *B dentium* (data not shown). To determine the functional impact of *B dentium* colonization on enterochromaffin-produced serotonin, we assessed 5-HT concentrations by immunostaining, qPCR, and LC-MS/MS. Increased numbers of 5-HT–positive cells were observed in both the ileum and colon of *B dentium* mono-associated mice relative to germ-free and heat-killed *B dentium*–treated mice (Figure 3*A* and *B*). Increases in 5-HT were observed in enteroendocrine cells directly above enteric neurons (Figure 3*C*). TPH-1 is the rate limiting enzyme for 5-HT production in enterochromaffin cells. The results of the immunostaining were corroborated by the significant increase in *Tph-1* expression in both the ileum and colon of *B dentium*
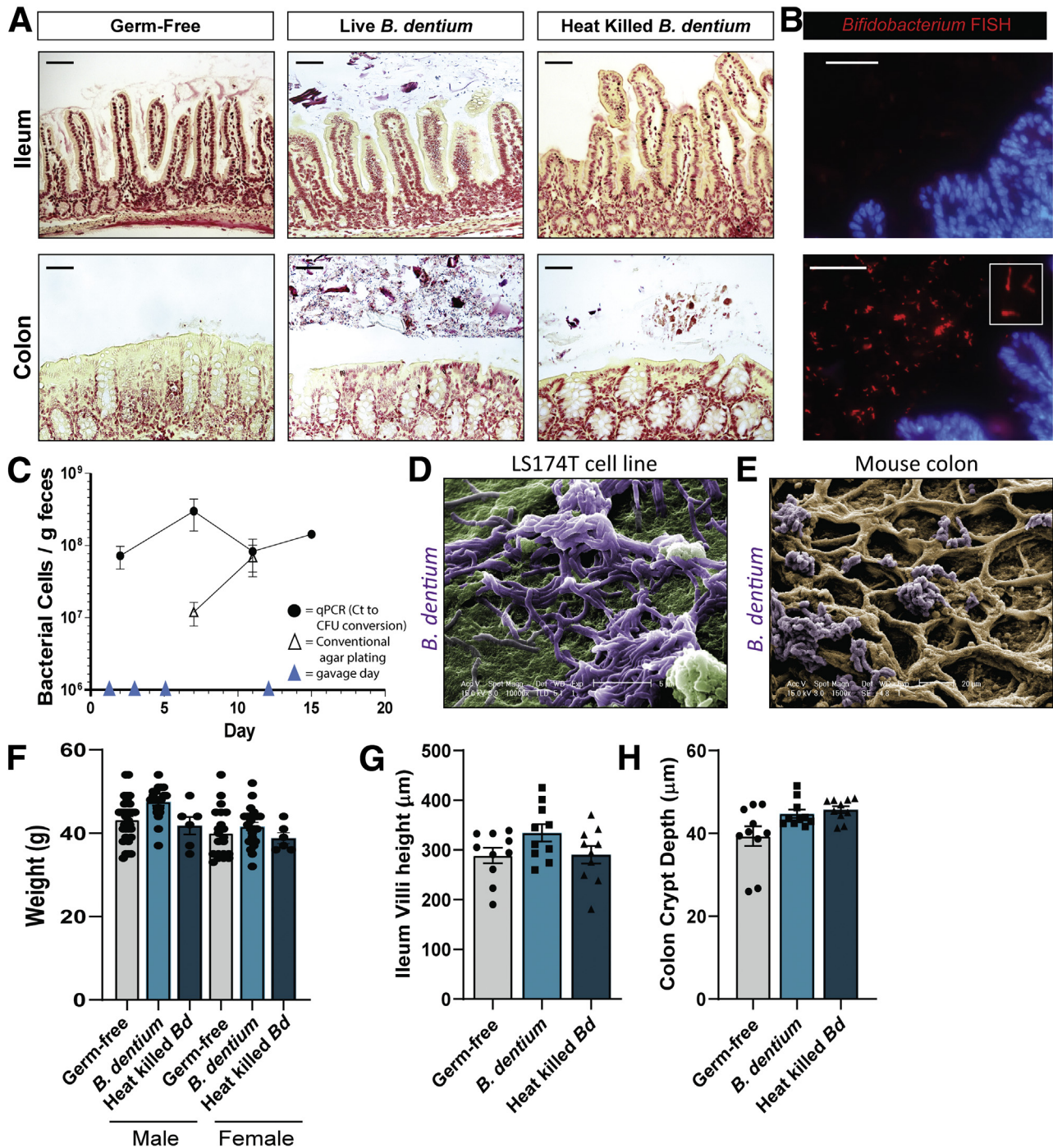
Figure 1. B dentium colonizes the adult germ-free mouse intestine. (A) Representative images of tissue Gram stain showing colonization of the ileum and colon in *B dentium*–colonized mice (n = 20) and the absence of bacterial cells in germ-free mice (n = 20). Sparse y-shaped *Bifidobacteria* cells were observed in heat-killed *B dentium*–treated mice (n = 10). Scale bar: 50 μm. (B) Representative images of FISH of colon tissue probed with Bifidobacterium genus–specific probe (Bif164) in both germ-free and *B dentium*–colonized mice. Host nuclei were counterstained with 4′,6-diamidino-2-phenylindole. Scale bar: 50 μm. (C) Quantitative results of *B dentium* colonization as measured by both qPCR and conventional agar plating of feces from colonized mice. (D) Representative scanning electron micrographs of *B dentium* (falsely colored in purple) adhering to human colonic mucin-producing LS174 cells (n = 3 replicates, 3 independent experiments). Scale bar: 5 μm. (E) Representative scanning electron micrographs of *B dentium* (falsely colored in purple) in *B dentium* mono-associated mouse colon (n = 3 per group). Scale bar: 20 μm. (F) Mouse weight in grams at day 17 (germ-free: n = 20 males, n = 20 females; live *B dentium*: n = 20 males, n = 20 females; and heat-killed *B dentium*: n = 6 males, n = 6 females). Analysis of (G) villus height in the ileum and (H) crypt depth in the colon of treated mice (germ-free: n = 5 males, n = 5 females; live *B dentium*: n = 5 males, n = 5 females; and heat-killed *B dentium*: n = 5 males, n = 5 females). Bd, *B dentium*.

mono-associated mice relative to germ-free and heat-killed *B dentium*–treated mice (Figure 3D). Increased *Tph-1* gene expression also was accompanied by

significantly increased 5-HT concentrations in the intestinal lumen of mice, as measured by LC-MS/MS (Figure 3E). Other groups have found that colonization
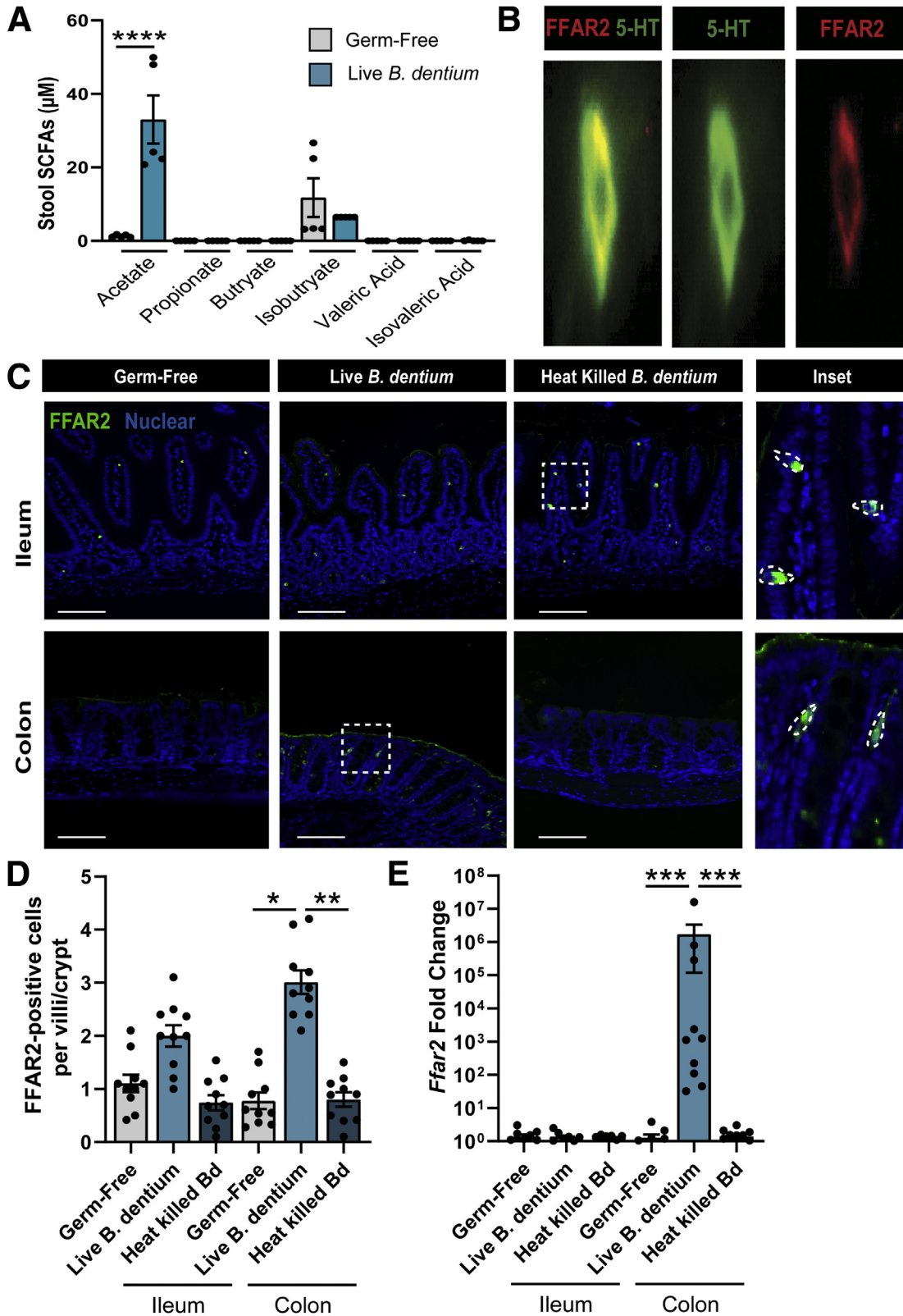
by a complex gut microbiota increases the number of 5-HT–positive cells, without changing the total number of enterochromaffin cells.[18] To examine the distribution of enterochromaffin cells within our model, we examined the levels of chromogranin A (ChgA), the gold standard for identification of enterochromaffin cells, by qPCR (Figure 3F) and immunostaining quantification (Figure 3G). In our model, no significant changes were observed in enterochromaffin expression or cell numbers between groups. However, we did observe increased numbers of 5-HT–positive ChgA-positive enterochromaffin cells (Figure 3H). Taken together, these results indicate that *B dentium* colonization increases the number of 5-HT–positive enterochromaffin cells and increases intestinal 5-HT.

Not All Commensal Microbes Promote Serotonin Production

To confirm that modulation of serotonin was not a ubiquitous feature of gut microbes, we mono-associated mice with another commensal microbe, *B ovatus*. Previous studies have found that mono-association with *Bacteroides thetaiotaomicron* did not influence serotonin.[18] Thus, we predicted that mono-association of a closely related *Bacteroides* would confirm that not all microbes modulate intestinal serotonin. Colonization of germ-free mice with *B ovatus* was confirmed by PCR with a *B ovatus*–specific primer and BHI agar plating. Interestingly, we observed no changes in 5-HT by immunostaining and quantification in the ileum or colon of *B ovatus* mono-associated mice compared with germ-free controls (Figure 4A and B). We also found no changes in *Tph-1* or serotonin levels between groups (Figure 4C and D). LC-MS/MS analysis showed that *B ovatus* mono-associated stool harbored 4 times lower concentrations of acetate (8.7 ± 7.0 μM) than *B dentium* mono-associated stool (33.0 ± 16.6 μM) (Figure 4E). However, moderate levels of propionate (15.2 ± 2.6 μM) were observed in *B ovatus*–treated stool. No changes were observed in other SCFAs. This is consistent with the KEGG pathway for *B ovatus*, which indicates that *B ovatus* has the genes to produce acetate (EC1.8.1.4) and propionate (EC2.7.2.1) (KEGG). Consistent with our *B dentium* mono-associated mice, we saw no change in ChgA expression or the number of enterochromaffin cells quantified from immunostaining in *B ovatus*–treated mice compared with germ-free controls (Figure 4F and G). As a result, the number of 5-HT–positive ChgA-positive cells were the same between *B ovatus* and germ-free groups (Figure 4H). These

findings suggest that not all bacteria are able to promote serotonin production in vivo.

B dentium *Stimulates 5-HT Production by Enterochromaffin Cells*

Although 5-HT is known to be produced by enterochromaffin cells, it also can be released from mast cells and neurons.[77–80] To determine if *B dentium*–secreted products, including acetate, were capable of stimulating 5-HT release specifically from enterochromaffin cells, ileal enteroid cultures were generated from adult Swiss Webster mice. These cultures of primary epithelial cells enable examination of epithelial responses independent from other cell and tissues types. *B dentium* was cultured in a fully defined media termed LDM4 and filtered through a 3-kilodalton filter to collect low-molecular-weight compounds, such as acetate. This filtered, spent media was termed *B dentium* CM. Enteroids were microinjected with either sterile control LDM4 media, *B dentium* CM, heat-killed *B dentium*, *B ovatus* CM, 5 mmol/L acetate, or 100 ng/mL LPS and incubated overnight. 5-HT concentrations present in the enteroid media were assessed by LC-MS/MS, and 5-HT–positive enterochromaffin cells were visualized by immunostaining. Immunostaining confirmed the presence of 5-HT–positive enterochromaffin cells in both control LDM4 media-injected enteroids and those microinjected with 50% *B dentium* CM (Figure 5A).

Importantly, injection of uninoculated bacterial media (LDM4) also was found to have no effect on the release of 5-HT. In contrast, addition of increasing concentrations of *B dentium* CM (5%–50%) resulted in a dose-dependent increase in the release of 5-HT from mouse ileal enteroids as determined by LC-MS/MS (Figure 5B). Injection of 10% *B dentium* CM was sufficient to observe an increase in release of 5-HT, although 50% *B dentium* CM resulted in the greatest stimulation of 5-HT release from mouse ileal enteroids. Likewise, addition of acetate stimulated 5-HT release, albeit not to the same extent as the conditioned media. To determine the specificity of the 5-HT release, enteroids were microinjected with LPS, 10^6 heat-killed *B dentium*, or 50% *B ovatus* CM. Unlike *B dentium* CM or microinjected acetate, LPS, 10^6 heat-killed *B dentium*, or 50% *B ovatus* CM had no effect on 5-HT release (Figure 5B), indicating that 5-HT release was not a general host response to the presence of bacteria. Addition of *B dentium* CM did not hinder enteroid viability (Figure 5C). Interestingly, we found that greater percentages of *B dentium* CM enhanced

---

Figure 2. (*See previous page*). B dentium mono-associated mice harbor increased acetate concentrations and colonic expression of the acetate receptor FFAR2. (*A* and *B*) *Bars* show variation in SCFA concentrations (ng/m*L*) in feces of germ-free and live *B dentium* mono-associated mice (n = 5/group). (*B*) Representative enlarged image of enterochromaffin cells from a germ-free mouse, *showing* co-expression of FFAR2 on 5-HT–positive cells within the intestine. (*C*) Representative images of ileum and colon tissue from germ-free, live *B dentium* mono-associated and heat-killed *B dentium*–treated mice stained with an anti-FFAR2 antibody. Host nuclei were counterstained with 4′,6-diamidino-2-phenylindole. *Inset shows* the classic enteroendocrine cell shape of FFAR2-positive cells, outlined in white. *Scale bar: 100 μm.* (*D*) Quantification of the number of FFAR2-positive cells identified per villi/crypt in the ileum or per crypt in the colon of treated mice (n = 10/group). (*E*) Relative fold change in ileal and colonic expression of the FFAR2 gene in germ-free, live *B dentium* mono-associated or heat-killed *B dentium* mice as measured by qPCR (n = 10/group). All data are presented as means ± SD. *$P < .05$, **$P < .01$, ***$P < .001$, ****$P < .0001$. Bd, *B dentium*.

viability as determined by trypan blue staining. We postulate this effect may be attributed to known anti-apoptotic effects of *Bifidobacterium* species on the intestinal epithelium.[81,82] Finally, to confirm the SCFA levels in our media, we examined *B dentium*– and *B ovatus*–conditioned media by LC-MS/MS. Similar to our stool levels, we observed that *B*

dentium secreted high levels of acetate in vitro, whereas *B ovatus* secreted low levels of acetate and propionate (Figure 5D).

To confirm these findings in a human model, we used HIEs. Similar to mouse enteroids, HIEs harbor a population of enterochromaffin cells, as seen by 5-HT immunostaining
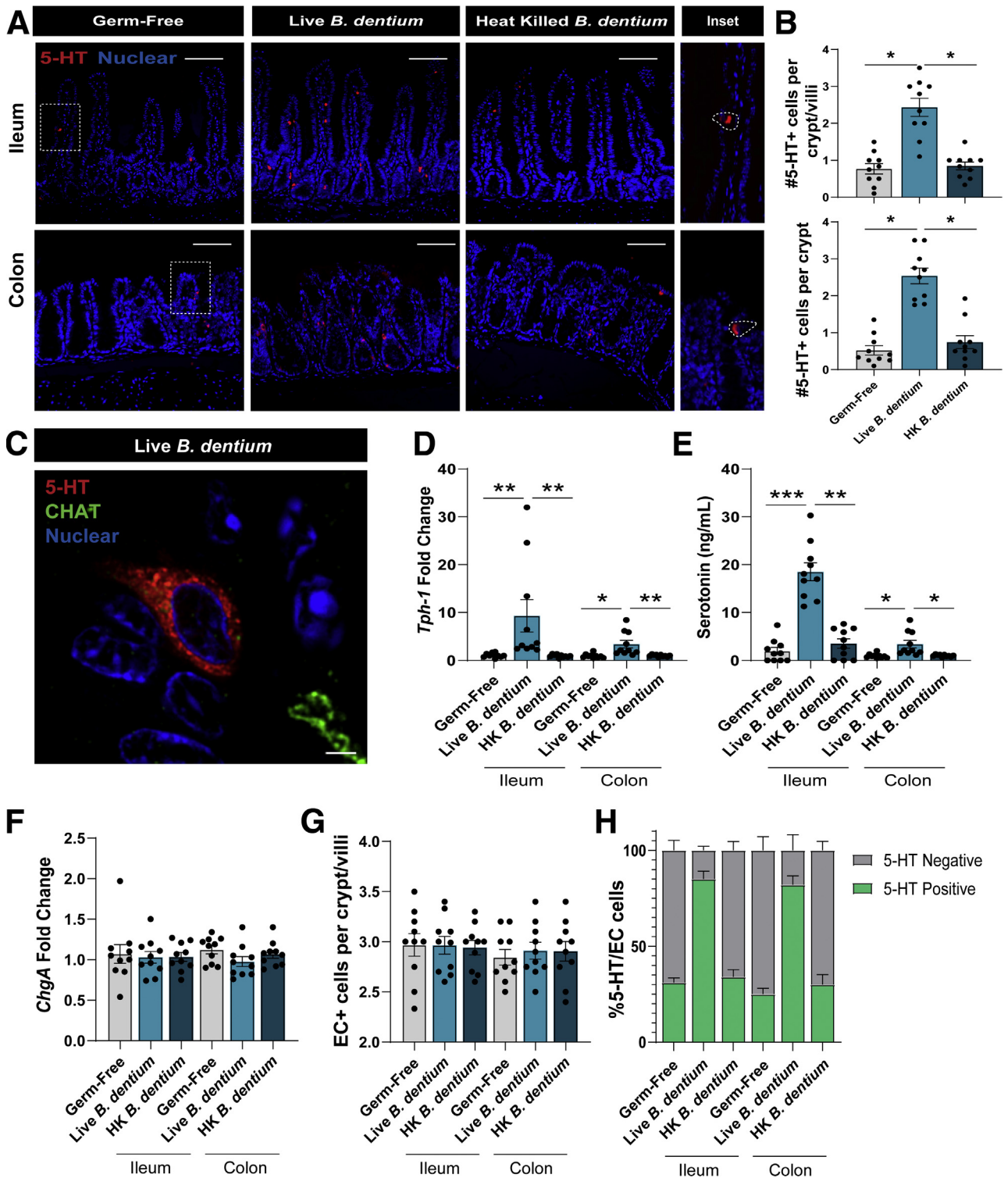
(Figure 6A). Three-dimensional HIEs were microinjected with 50% uninoculated LDM4, 50% *B dentium* CM, 10^6 heat-killed *B dentium,* or 5 mmol/L acetate. As observed in our mouse enteroids, HIEs treated with *B dentium* CM and, to a lesser degree, acetate had increased levels of 5-HT by LC-MS/MS compared with HIEs treated with media, LDM4, and heat-killed bacteria controls (Figure 6B). Increased viability in 3D HIEs was observed only with the addition of *B dentium* CM, as assessed by trypan blue staining. We also used 2D HIE monolayers with the same treatment regimen. As expected, we observed increased levels of released 5-HT after incubation with *B dentium* CM or acetate (Figure 6C). In 2D format, we did not observe changes in cell viability with any treatments.

Because enterochromaffin cells represent a small population, we sought to fine-tune the number of enterochromaffin cells, and thus the sensitivity of our assay, by using tet*NGN3*-HIEs.[46] These HIEs can be induced to overexpress *NGN3*, a transcription factor that promotes epithelial differentiation into enteroendocrine lineages.[46,83–86] In this inducible model system of the human intestinal epithelium, >50% of the cells become enterochromaffin cells as confirmed by 5-HT immunostaining (Figure 6D). Microinjection of 50% *B dentium* CM into 3D tet*NGN3*-HIEs resulted in significantly increased release of 5-HT (Figure 6E). Similar to our results from enteroids derived from mouse ileum, microinjection of acetate resulted in stimulation of 5-HT release. The release of 5-HT in tet*NGN3* HIEs was approximately 4-fold greater than what was observed in wild-type mouse enteroids. We also observed enhanced viability with administration of *B dentium* CM. Consistent with 3D enteroids, 2D monolayers of tet*NGN3* HIEs released increased 5-HT when exposed to *B dentium* CM (Figure 6F). We also observed 5-HT release in response to acetate, although these levels were far below that of *B dentium* CM. To ascertain the role of acetate in *B dentium*–stimulated release of 5-HT, we removed acetate in the CM by converting it back to acetyl-Co-A. Loss of acetate in our modified *B dentium* CM reduced the ability of CM to stimulate increased 5-HT release as observed with *B dentium* CM. However, levels of 5-HT still were greater than in media and LDM4 controls, indicating that other *B dentium* metabolites contribute to 5-HT release. No changes were observed in viability in this 2D format as well. These data show that *B*

dentium–secreted products, including acetate, can modulate 5-HT production by host enterochromaffin cells.

The 5-HT Reuptake Transporter SERT and Specific 5-HT Receptors Are Up-Regulated by B dentium

Once released, 5-HT can interact with multiple isoforms of the 5-HT receptor present on various cell types within the intestine. Increased local concentrations of 5-HT may impact the expression of these receptors. Therefore, we examined whether 5-HT–receptor expression was affected in our live *B dentium* in vivo model via qPCR. We found that expression of the colonic 5-HT receptors 2a and 4 (*Htr2a* and *Htr4*) were increased significantly in *B dentium* mono-associated mice (Figure 7A). This approximately 10-fold up-regulation of *Htr2a* and *Htr4* receptors indicates the expected coordinated physiological response to 5-HT release.

In addition to interacting with receptors, 5-HT can be transported into neighboring enterocytes or neurons via the 5-HT reuptake transporter (SERT). We examined the impact of *B dentium*–secreted products on SERT levels by immunostaining and qPCR in vivo and in our enteroid models. Immunofluorescence staining was used to examine the SERT protein in tissue sections, showing an increased fluorescence signal in both the ileum and colon of *B dentium* mono-associated mice relative to controls (Figure 7B). *B dentium* mono-associated mice yielded significantly increased expression of *Sert* mRNA in both the ileum and colon relative to germ-free mice (Figure 7C). Increased epithelial SERT was mirrored in enteroids microinjected with *B dentium* CM. *B dentium* CM (10%–50%), but not acetate, stimulated dose-dependent increases in *Sert* mRNA expression (Figure 7D) and SERT protein (Figure 7E). These data suggest that *B dentium* secretes other product(s) besides acetate, capable of up-regulating SERT.

B dentium Increases Hippocampal 5-HT–Receptor Expression and Partially Restores 5-HT–Dependent Behavior

To determine if *B dentium* colonization could alter the central nervous system (CNS) serotonergic system we examined serotonin-receptor expression in the brains of

---

Figure 3. (*See previous page*). *B dentium* mono-associated mice have higher levels of 5-HT–positive enterochromaffin cells and luminal serotonin. (*A*) Representative images of ileum and colon tissue stained with an anti–5-HT antibody showing both increased staining intensity in enterochromaffin cells in *B dentium* mono-associated mice. Host nuclei were counterstained with 4′,6-diamidino-2-phenylindole. Inset shows the classic enterochromaffin cell shape of 5-HT–positive cells, outlined in white. Scale bar: 100 μm. (*B*) Quantification of the number of 5-HT–positive cells identified per villi/crypt in the ileum or per crypt in the colon of treated mice (n = 10/group). (*C*) Representative image of 5-HT–positive enterochromaffin cell in close proximity to a CHAT-stained enteric neuron in a live *B dentium*–treated mouse ileum. *Scale bar*: 10 μm. (*D*) Relative fold changes in expression of *Thp-1* in the ileum and colon of germ-free, live *B dentium* mono-associated and heat-killed *B dentium* mice (n = 10/group). (*E*) Serotonin concentrations (ng/mL) in the lumen of the ileum and colon (n = 10/group) as measured via mass spectrometry. (*F*) Relative fold change in expression of *ChgA* in ileal and colonic tissue in germ-free, live, *B dentium* mono-associated and heat-killed *B dentium*–treated mice (n = 10/group) as measured via qPCR. (*G*) Quantification of the number of ChgA-positive cells identified per villi/crypt in the ileum or per crypt in the colon of treated mice (n = 10/group). (*H*) Quantification of the number of cells that co-stain for 5-HT and ChgA (5-HT–positive/ChgA-positive cells) identified per villi/crypt in the ileum or per crypt in the colon of treated mice (n = 10/group). All data are presented as means ± SD. *P < .05, **P < .01, ***P < .001. CHAT, choline acetyltransferase; EC, enterochromaffin cell.
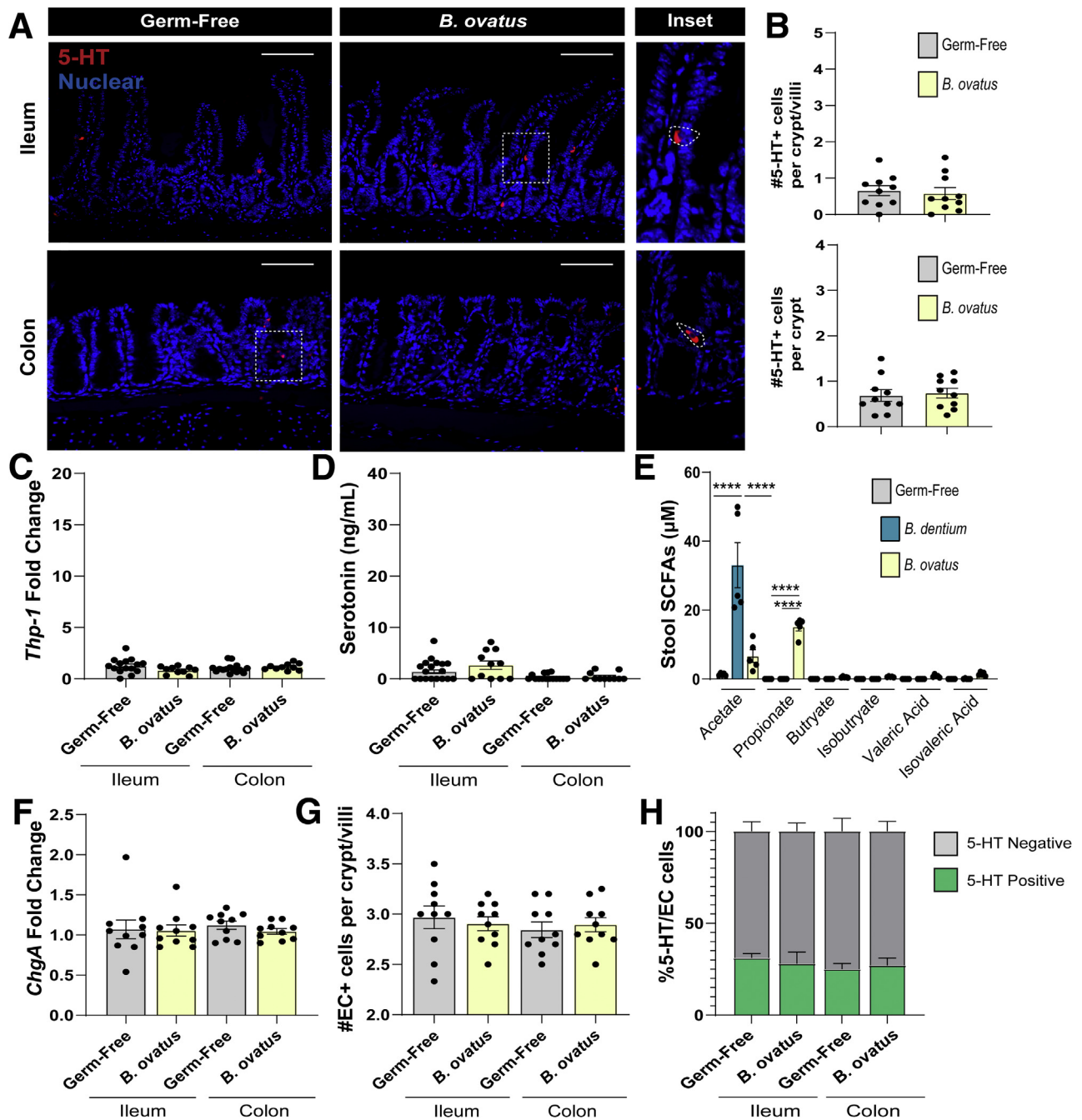
Figure 4. *B ovatus* mono-associated mice show no changes in 5-HT staining or luminal concentrations. (*A*) Representative images of ileum and colon tissue stained with an anti–5-HT antibody in germ-free and *B ovatus* mono-associated mice. Host nuclei were counterstained with 4′,6-diamidino-2-phenylindole. Insets show the classic enterochromaffin cell shape of 5-HT–positive cells (white outline). Scale bar: 100 μm. (*B*) Quantification of the number of 5-HT–positive cells identified per villi/crypt in the ileum or per crypt in the colon of treated mice (n = 10/group). (*C*) Relative fold changes in expression of *Thp-1* in the ileum and colon of germ-free or live *B ovatus* mice (n = 10/group). (*D*) Serotonin concentrations (ng/mL) in the lumen of the ileum and colon (n = 10/group) as measured via mass spectrometry. (*E*) SCFA LC-MS/MS analysis of germ-free, live *B dentium* and live *B ovatus*–treated mouse stool. (*F*) Relative fold change in expression of ChgA in ileal and colonic tissue in germ-free or live *B ovatus* mono-associated mice (n = 10/group) as measured via qPCR. (*G*) Quantification of the number of ChgA-positive cells identified per villi/crypt in the ileum or per crypt in the colon of treated mice (n = 10/group). (*H*) Quantification of the number of cells that co-stain for 5-HT and ChgA (5-HT–positive/ChgA-positive cells) identified per villi/crypt in the ileum or per crypt in the colon of treated mice (n = 10/group). All data are presented as means ± SD. ****$P < .0001$. EC, enterochromaffin cell.
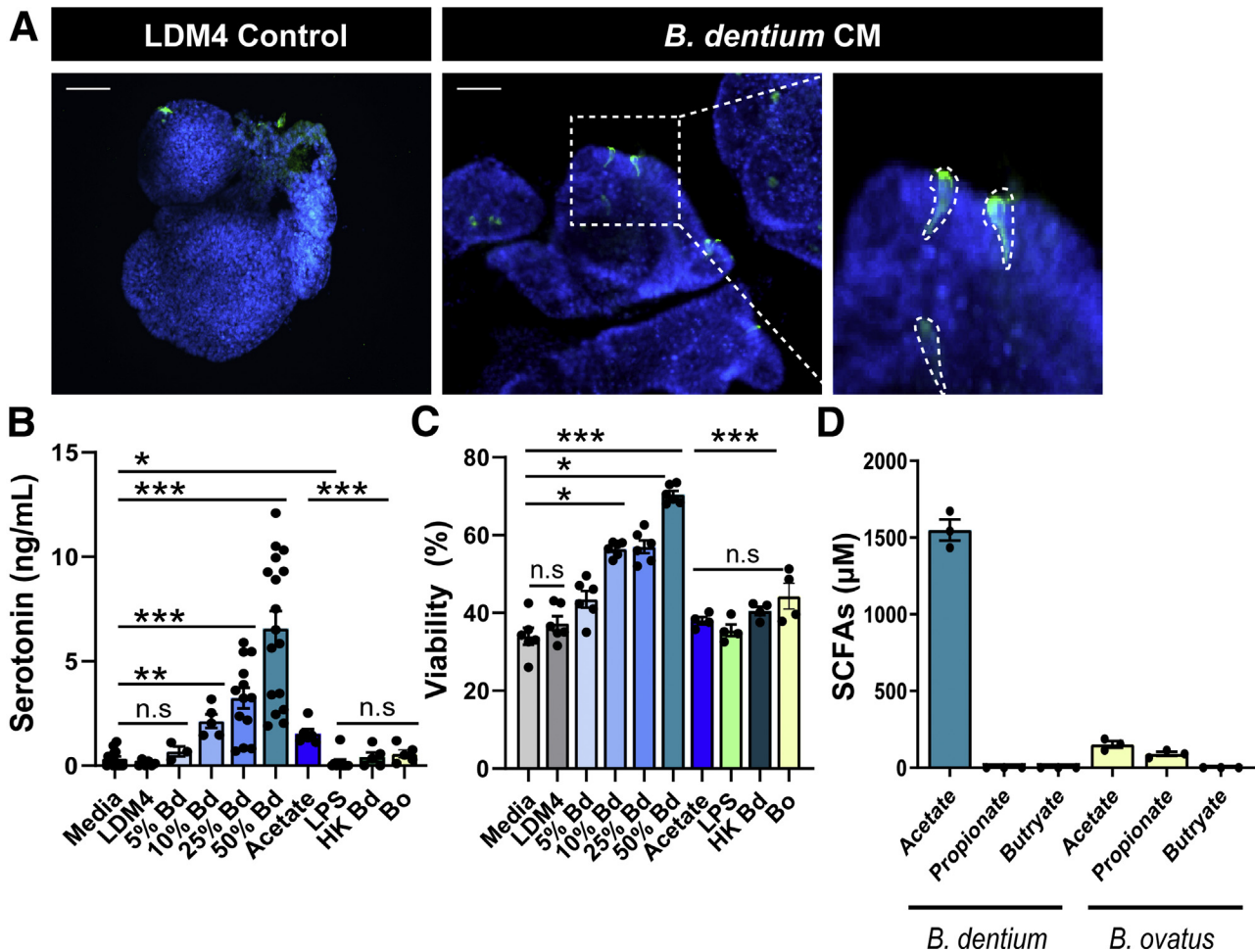
Figure 5. *B dentium CM* stimulates 5-HT release from enterochromaffin cells in mouse enteroids. (*A*) Representative images of immunostaining in ileal enteroids, indicating the presence of 5-HT–positive enterochromaffin cells. *Inset* is image enlarged from original showing enterochromaffin cell morphology and staining pattern. Host nuclei were counterstained with 4′,6-diamidino-2-phenylindole. Scale bar: 50 μm. (*B*) *Bars* represent serotonin concentrations released into media from ileal enteroids microinjected with media, 50% uninoculated LDM4, increasing concentrations of *B dentium* LDM4 *CM* (5%–50%), 50% *B ovatus CM*, 5 mmol/L acetate, 10^6 heat-killed *B dentium,* or 100 ng/mL LPS (n = 3 wells/group, 4 independent experiments). (*C*) Enteroid viability as measured via trypan blue staining (4 wells/treatment, 4 independent experiments). Data are expressed as *the* percent*age of* viable cells relative to total. (*D*) SCFA LC-MS/MS analysis of *B dentium* and *B ovatus CM*. All data are presented as means ± *SD*. *$P < .05$, **$P < .01$, ***$P < .001$. BD, *B dentium* conditioned media; HK Bd, heat-killed *B dentium*; Bo, *B ovatus* conditioned media.

germ-free and *B dentium* mono-associated mice. Based on the significant up-regulation observed in the gut, and its known role in behavioral processes, we focused on expression of the excitatory serotonin receptor *Htr2a* using RNA ISH. Expression of *Htr2a* was assessed in the hippocampus and characterized by hippocampal region (dentate gyrus, CA1, CA2, and CA3) and by strength of expression (Figure 8*A*). Cells were categorized as weak, media, or strongly expressing based on fluorescence intensity as previously established[65] (Figure 8*B*). *B dentium* mono-associated mice were observed to have significantly increased expression of *Htr2a* in the CA1 region of the hippocampus relative to germ-free animals, although no significant differences were detected in the other hippocampal regions examined (Figure 8*C*). More specifically, a

significant increase in the percentage of cells in the strong or media levels of *Htr2a* in the CA1 region was observed.

We next sought to define if *B dentium*–mediated changes in the CNS serotonergic system also would result in behavioral changes. Previous studies with germ-free mice have established that these mice show an abnormal, "anxiolytic" or reduced-anxiety phenotype, as well as an increased propensity to engage in repetitive behaviors such as grooming.[14,22,87–90] The marble burying test is a simple test that is used commonly to quantify repetitive and/or anxiety-like behavior in rodents, but also is associated with typical mouse digging behavior.[91–96] This test has been used previously to test 5-HT active compounds such as selective serotonin re-uptake inhibitors.[91] Furthermore, the 5-HT2A–receptor antagonist YM992 has been shown to
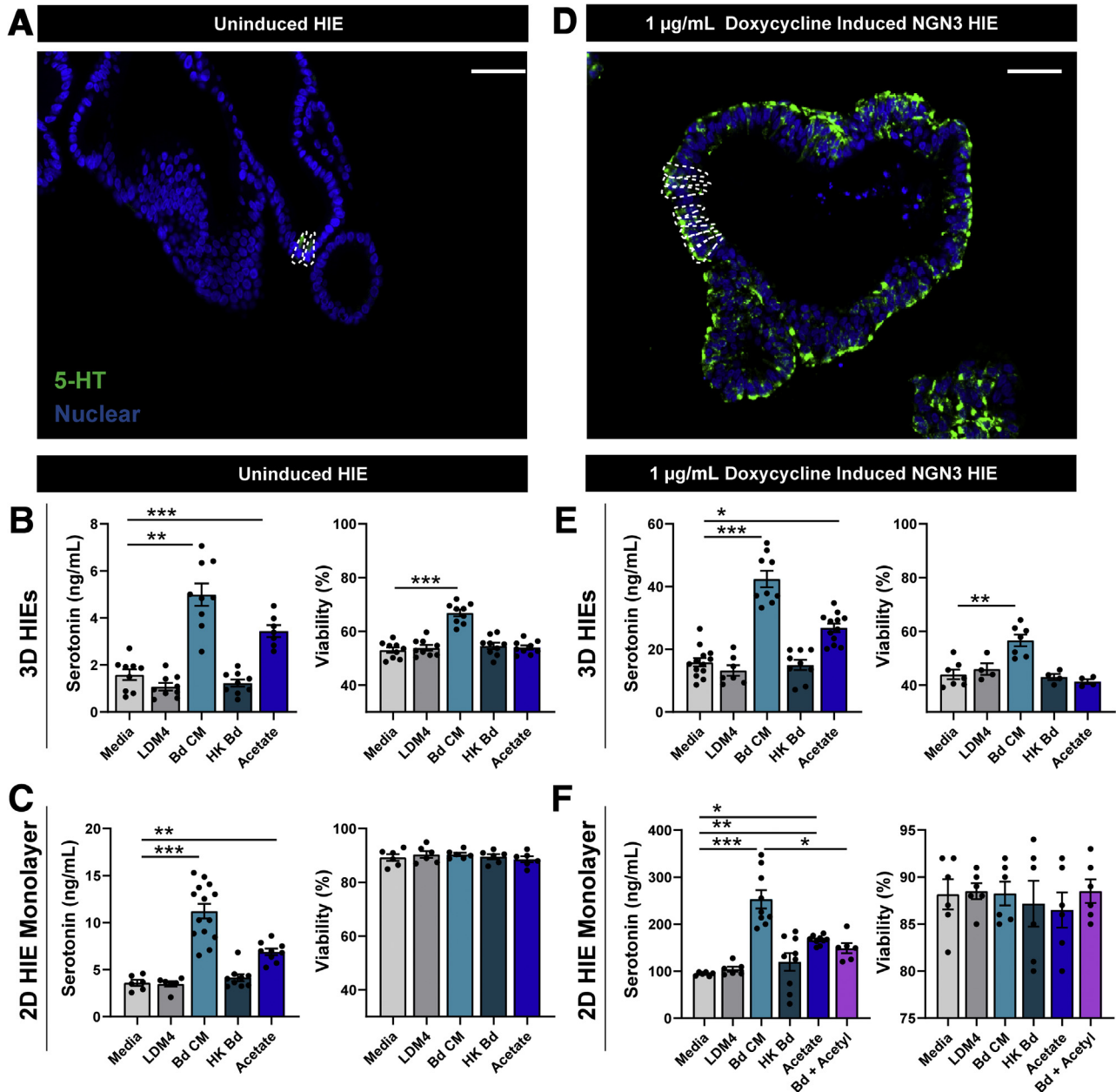
Figure 6. *B dentium* **CM stimulates release of increased 5-HT from HIEs and tetNGN3 HIE models.** (*A*) Representative images of immunostaining in jejunal HIEs, indicating the presence of 5-HT–positive enterochromaffin cells. White outlines highlight enterochromaffin cells. Host nuclei were counterstained with 4′,6-diamidino-2-phenylindole. Scale bar: 100 μm. (*B*) Bars represent serotonin concentrations in enteroid media after microinjection of 3D HIEs with media, 50% uninoculated LDM4, 50% *B dentium* CM, 10^6 heat-killed *B dentium*, or 5 mmol/L acetate (left) and enteroid viability as measured via trypan blue staining (right) (n = 3 wells/group; 3 independent experiments). (*C*) Bars represent serotonin concentrations in 2D enteroid monolayer media after incubation with the same treatment groups and enteroid viability as measured via trypan blue staining (right) (n = 3 wells/group; 3 independent experiments). (*D*) Representative images of immunostaining in jejunal tetNGN3 HIEs, induced with 1 μg/mL doxycycline to drive enteroendocrine cell fate. 5-HT–positive enterochromaffin cells are found all over the enteroids, with some enterochromaffin cells outlined in white to highlight cell shape. Host nuclei were counterstained with 4′,6-diamidino-2-phenylindole. Scale bar: 50 μm. (*E*) Bars represent serotonin concentrations in media after microinjection of 3D tetNGN3 HIEs with media, 50% uninoculated LDM4, 50% *B dentium* CM, 10^6 heat-killed *B dentium*, or 5 mmol/L acetate (left) and enteroid viability as measured via trypan blue staining (right) (n = 3 wells/group; 3 independent experiments). (*F*) Bars represent serotonin concentrations in 2D tetNGN3 HIE monolayer media after incubation with the same treatment groups and enteroid viability as measured via trypan blue staining (right) (n = 3 wells/group; 3 independent experiments). All data are presented as means ± SD. *$P < .05$, **$P < .01$, ***$P < .001$. BD CM, *B dentium* conditioned media; HK Bd, heat-killed *B dentium*.
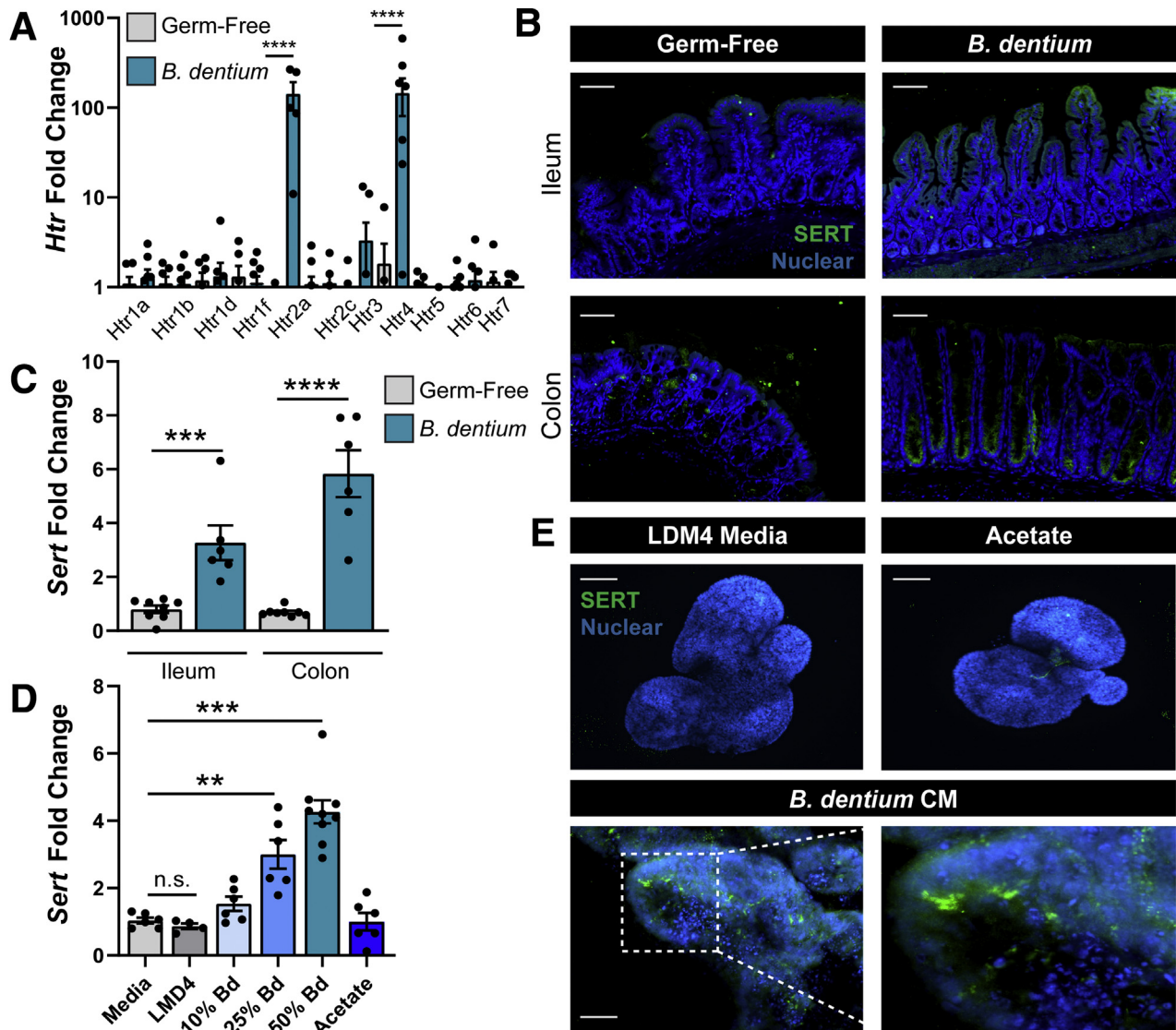
Figure 7. **B dentium** up-regulates expression of specific 5-HT receptors and the 5-HT reuptake transporter (SERT). (*A*) Relative fold change in expression of the major 5-HT receptors within the germ-free and *B dentium* mono-associated mouse colon by qPCR (n = 8/group). (*B*) Representative images of SERT immunostaining in ileum and colon of germ-free and live *B dentium* mono-associated mice. Host nuclei were counterstained with 4′,6-diamidino-2-phenylindole. Scale bar: 100 μm. (*C*) Relative fold change in expression of *Sert* within the germ-free and *B dentium* mono-associated mouse ileum and colon (n = 7–10/group). (*D*) Relative fold change in expression of *Sert* in mouse enteroids microinjected with LDM4 control media, 50% *B dentium* CM, or 5 mmol/L acetate (n = 3/treatment group, 3 independent experiments). (*E*) Representative images of SERT immunostaining in mouse enteroids microinjected with media, 50% LDM4, 10%–50% *B dentium* CM, or 5 mmol/L acetate. Scale bar: 100 μm. Inset shows enlarged image of increased staining in enteroids injected with *B dentium* CM. Host nuclei were counterstained with 4′,6-diamidino-2-phenylindole. All data are presented as means ± SD. **$P < .01$, ***$P < .001$, ****$P < .0001$.

reduce marble burying, further implicating the association between microbial-induced modulation of this receptor and the behavioral changes observed.[91–96] Swiss Webster mice with a complete gut microbiota (SPF) buried on average 25% (25.5% ± 4.5%) of the marbles encountered during the test (Figure 8D and E). In contrast, germ-free mice buried significantly fewer marbles (6.8% ± 1.1%) relative to the SPF cohort. *B dentium* monocolonized mice buried a significantly higher percentage (15.8% ± 3.5%) of

marbles than germ-free mice, but not as many as the SPF cohort. These data suggest that the reduced-anxiety phenotype observed in germ-free mice was partially normalized by the monocolonization with *B dentium*, even though this colonization was short term and was performed later in life.

To confirm that our observed marble burying phenotype was not caused by differences in locomotor coordination between germ-free compared with *B dentium* mono-
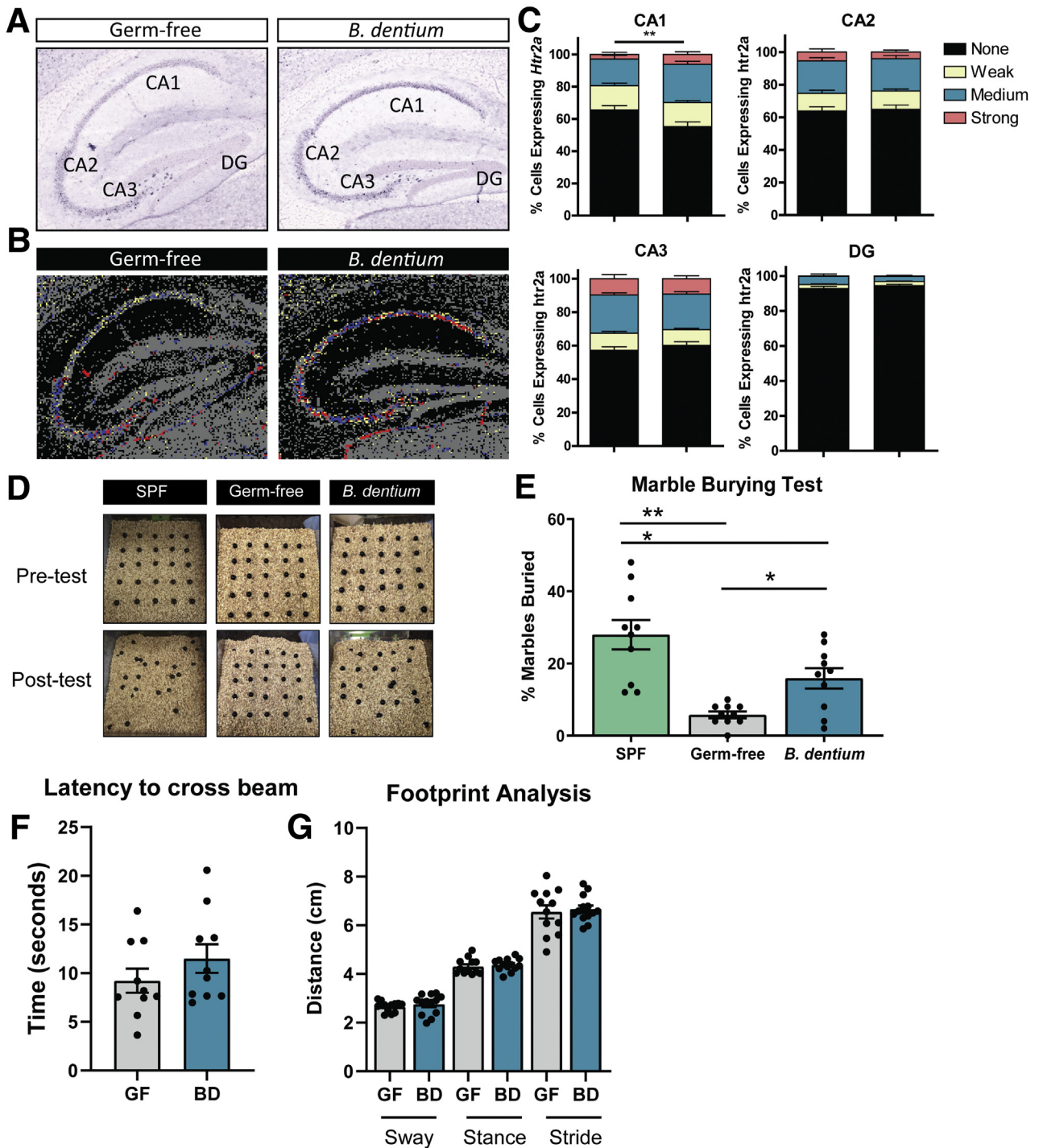
Figure 8. *B dentium* increases hippocampal expression of *Htr2a* and normalizes behavior. (*A*) Representative images of the *Htr2a* in situ hybridization staining within the hippocampal formation of germ-free and *B dentium* mono-associated mice. (*B*) Representative images of cells categorized as expressing *Htr2a* with cells labeled as strong (red), media (yellow), weak (blue), or no expression (black). (*C*) *Bars* represent cells categorized as strong, media, weakly, or not expressing *Htr2a* in each region of the hippocampal formation (CA1, CA2, CA3, dentate gyrus [DG]) (n = 4 sections/mouse with n = 5–6/group). (*D*) Representative images of marble bury test before (*upper panel*) and after (*lower panel*) the test. (*E*) *Bars* represent the percentage of total marbles buried during the test by mice in each treatment group (n = 10–13/group). (*F*) *Bars* represent time taken by mice to cross a beam in the balance beam test (n = 10/group). (*G*) Footprint analysis showing the sway, stance, and stride measurements (distance in cm) averaged for each mouse (n = 10–12/group). BD, *B dentium*; GF, germ-free.

associated mice, we also assessed locomotion using the balance beam test (Figure 8F) and footprint analysis (Figure 8G). No differences were observed between germ-free and live *B dentium* mono-associated mice, suggesting that monocolonization does not affect motor coordination. These findings add to our previous work, which found no difference in overall motor activity between *Bifidobacterium*-colonized mice and germ-free in the open field test.[24] Overall, these data show that *B dentium* modulates the serotonergic system in both the intestine and the brain. This modulation likely influences behavior, and suggests that supplementation with a single, carefully selected, bacterial strain may be able to partially rescue behavioral deficits induced by shifts in the intestinal microbiota. These data further highlight the importance of *Bifidobacterium* species, and specifically *B dentium*, in the adult microbiome–gut–brain axis.

Discussion

Recent studies have highlighted a role for the gut microbiota in regulation of 5-HT[18]; however, the mechanism(s) for this regulation was previously unclear. Herein, we show that mono-association of animals with the commensal *B dentium* significantly modulates the host serotonergic system. Our findings indicate that *B dentium* colonizes the intestinal mucus layer where it delivers secreted metabolites, such as acetate, to the underlying epithelium. Consistent with other reports, we have confirmed that acetate is capable of stimulating enterochromaffin cells to secrete 5-HT.[25,32,33,36] We have extended these previous findings that rely largely on cancer-based cell lines and ex vivo methods by using mouse and human intestinal enteroid cultures, which more closely recapitulate the intestinal epithelium. We also show that *B dentium*–secreted products apart from acetate are capable of stimulating 5-HT release. We included heat-killed *B dentium* and commensal *B ovatus* in our study to show that select viable gut microbes modulate 5-HT. This work shows that generation of microbial compounds, including acetate, by a single bacterial species modulates 5-HT production in a gnotobiotic mouse model. In addition to the increased production and release of 5-HT, mice mono-associated with *B dentium* showed increased expression of select 5-HT receptors in both the gut and the brain, which may modulate several downstream signaling targets. As a result, *B dentium* may represent a next-generation category of probiotics capable of modulating 5-HT and the microbiome–gut–brain axis.

Enteroid cell cultures confirmed that both *B dentium* and acetate elicit 5-HT release from enterochromaffin cells within the intestinal epithelium. This is consistent with findings from other groups that have noted that a complex gut microbiota regulates peripheral 5-HT concentrations.[17–20] Enterochromaffin cells act as chemical and mechanical transducers, serving to connect the intestinal environment and the enteric nervous system. Enterochromaffin cells respond to a number of stimuli in the luminal environment such as SCFAs, pH, oxygen, amino acids, monosaccharides, catecholamines (dopamine, epinephrine,

norepinephrine, γ-aminobutyric acid [GABA]), purines (adenosine and adenosine triphosphate), and mechanical stimuli.[73,75,97–102] Multiple groups have shown a role for SCFAs in the stimulation of 5-HT release.[25,32,36,73,103,104] Mouse enteroids (referred to in the literature by some as *intestinal organoids*) derived from small and large intestine have been shown to secrete 5-HT in response to acetate and propionate.[36]

By using ex vivo mouse ileum, Nzakizwanayo et al[105] found that secreted products from the acetate-producing *E coli* Nissle 1917 increased extracellular 5-HT concentrations. However, addition of another human gut commensal, *E coli* MG1655, which produces similar levels of acetate, was unable to stimulate 5-HT secretion. These findings implicate additional bacterial metabolites that perhaps work in coordination with acetate to stimulate 5-HT release. These findings are consistent with our work, which suggests that other *B dentium* metabolites also influence 5-HT release. Enterochromaffin cells also are responsive to GABA.[73] We previously showed that *B dentium* is capable of producing GABA,[42] and *B dentium*–produced GABA may contribute to 5-HT release in our model as well. Lactate is also known to activate GPR132 on enterochromaffin cells,[76] and the *B dentium* genome has annotated enzymes necessary for the fermentation of glucose and fructose to lactic acid.[72] As a result, lactate also could promote 5-HT from enterochromaffin cells. Enterochromaffin cells are known to express functional Toll-like receptors,[106] and addition of heat-killed *Lactobacillus brevis* SBC880, another lactic acid–producing bacteria, was shown to stimulate 5-HT release from EC-like RIN-14B cells and mouse small intestinal loops.[107] Our in vivo and in vitro work with heat-killed *B dentium* indicates that *B dentium* membrane components do not contribute to enterochromaffin cell release of 5-HT. At present, it is unclear what components of *B dentium* metabolites contribute to 5-HT stimulation, but this is an exciting area meriting future investigation

In addition to stimulation of 5-HT release, *B dentium* may be altering the conjugation of 5-HT, thereby contributing to the bioactive 5-HT pool. A substantial proportion of 5-HT found in germ-free mice exists as glucuronide-conjugated 5-HT.[20] In contrast, only 6% of 5-HT is glucuronide-conjugated in conventionalized mice (germ-free mice colonized with SPF feces). As a result, the majority (90%) of 5-HT exists in the bioactive state in conventionalized free mice, while germ-free mice have a deficit of bioactive 5-HT. Bacterial enzymes such as β-glucuronidase have been proposed to deconjugate 5-HT-O-glucuronide.[20] *B dentium* is known to show β-glucuronidase activity[108] and thus may be contributing to increased bioactivity of 5-HT.

Similar to other published findings examining microbial-induced 5-HT release,[18,20,103,109–115] we observed significant amounts of 5-HT secreted into the intestinal lumen in mice colonized with *B dentium* compared with germ-free controls. Once in the lumen, 5-HT can interact with other members of the gut microbiota. 5-HT has been documented to stimulate the growth of *E coli*, *Enterococcus faecalis*, and *Rhodospirillum*

rubrum in culture.[116,117] 5-HT also has been shown to serve as a quorum-sensing molecule in *Pseudomonas aeruginosa*.[118] To the best of our knowledge, no role has been identified previously for 5-HT in modulation of growth of *Bifidobacterium* species. However, during development, *Bifidobacterium* species act in various ways to prime the intestinal environment for subsequent colonizers, and they participate in several known interspecies cross-feeding relationships.[119,120] Modulation of 5-HT stores by *B dentium* therefore also may function in this capacity in adult animals, thereby influencing gut microbial composition.

5-HT is known to mediate several functions, including intestinal motility. TPH-2–deficient mice, which lack neuronal-generated 5-HT, show increased transit time and colonic motility. In addition, Spencer et al[121] found that colon peristalsis still could occur after removing the mucosa (and thus the enterochromaffin cells) from mouse and guinea pig colon, highlighting the importance of enteric nervous system (ENS) 5-HT for motility. Enterochromaffin 5-HT also has been shown to participate in colonic motility. TPH-1–deficient mice, which lack enterochromaffin-generated 5-HT, show slower in vitro propulsion of large fecal pellets and an absence of reflex activity in response to mucosal stimulation.[122] In our mice, we did not observe any changes in *Tph-2* mRNA or find noticeable differences in stool consistency (data not shown). However, no definitive colonic motility tests were performed, so at present it remains unclear whether colonic motility is altered in our mice. These are important considerations for future work.

Modulation of the gut–brain axis by the microbiome has long been linked to alterations in host behavior. Addition of other *Bifidobacterium* species affect various host behaviors, including repetitive and anxiety-like behaviors. For instance, supplementation of SPF mice and rats with commensal *Bifidobacterium longum* had anxiolytic effects,[123,124] whereas *Bifidobacterium infantis* alleviated depressive-like behaviors in a rat model of maternal separation.[125] Recently, *B longum* NCC3001 was found to improve depression scores and induce pronounced changes in brain activity in human patients with irritable bowel syndrome.[126] Our work also has shown that neonatal colonization with a consortium of human-derived *Bifidobacterium* species, including *B dentium*, affects adult rodent behavior including anxiety and hyperactivity.[24] These studies show that infant-type *Bifidobacteria* modulate select host behaviors via modifications to neurodevelopmental processes.[24,127] We hypothesized that *B dentium*–produced acetate stimulates local 5-HT production and release by enterochromaffin cells. We speculate that *B dentium*–mediated modulation of other components of the serotonergic system, such as 5-HT–receptor expression in both the gut and the brain, result in the behavioral changes observed. Because dysregulation of the serotonergic system is implicated in disease pathogenesis in both the gut and the brain, modulation of this system by a particular microbe may provide new strategies to target these disorders. 5-HT bioavailability and receptor expression has long been linked to behavior and has been shown to have effects on both repetitive behaviors as well as anxiety-like

behaviors.[128–133] Numerous studies using germ-free animals have shown that the gut microbiota influences anxiety-like behavior and that germ-free mice show decreased anxiety[14,22,87–89] and an increased stress response.[89,134] Colonization with microbes early in life has been shown to normalize these aberrant behaviors. We therefore predicted that *B dentium* mono-association may affect these behaviors via modulation of the host CNS serotonergic system. Our results show that germ-free mice show decreased species-typical anxiety behaviors and that colonization with a single bacterial species, in this case *B dentium*, partially normalizes anxiety-like behavior. We speculate that this may be owing to bacterial-induced changes to the serotonergic system.

Several studies have documented the ability of the microbiota as a whole to regulate the serotonergic system,[2,14,18,25,61,104,105,107,135] however, this study shows that the *Htr2a* is expressed differently in the brain based on the microbial-colonization status of the gut. Htr2a mediates excitatory neurotransmission[136] and Htr2a knockout mice show decreased anxiety.[137] Studies in Parkinson's disease patients also have identified an association between *HTR2A* expression and impulse control and repetitive behavior.[138] Although we speculate that *Htr2a* expression may be involved in our mouse behavior, our findings do not rule out the possibly that other signaling pathways are involved and HTR2A may not be the sole mediator of all our results. To assess the role of intestinal and neuronal HTR2A in mediating our behavior phenotype, region-specific Htr2a knockout mice could be used. These studies would definitively identify a role for HTR2A in *B dentium*–modulated behavior effects.

Several possible mechanisms may facilitate cross-talk between microbes and the CNS. Microbes have been shown to elicit signals to the CNS via the vagal nerve.[139,140] Supplementation of *B longum* was shown to have an anxiolytic effect in a model of chronic colitis and this effect was abrogated when mice were vagotomized before colitis.[141] The microbiota also has been shown to activate the mucosal immune system,[142] which may alter epithelial permeability, activate nociceptive sensory pathways, and dysregulate the ENS.[143] This may be through the production or stimulation of neurotransmitters such as 5-HT, GABA, histamine, melatonin, and acetylcholine, which can modulate afferent sensory nerves.[144,145] Our work indicates that certain metabolites produced by *Bifidobacterium*, such as acetate (a SCFA), can stimulate release of 5-HT, which may act peripherally or may stimulate the ENS directly. This connection supports recent literature, which documents release of 5-HT from enterochromaffin cell cultures treated with SCFAs.[18,25,32,36,73,103] Recent studies also have shown that bacterial peptidoglycan derived from the commensal gut microbiota can be translocated into the brain and sensed by specific pattern-recognition receptors of the innate immune system,[146] which may serve as a method of gut–brain communication. It is additionally possible that small-molecule bacterial proteins or metabolites may cross the blood-brain barrier and directly modify the host CNS.

Probiotic strains, particularly *Lactobacillus* and *Bifidobacterium* species, have been hypothesized to beneficially influence mammalian health and disease, via different signaling pathways including the serotonergic system.[147–152] Our findings support the modulation of the serotonergic system by a model gut microbe, *B dentium*, and provide a potential mechanism by which select microbes and their metabolites can promote endogenous, localized 5-HT biosynthesis. We speculate this may be an important bridging signal in the microbiome–gut–brain axis.

Materials and Methods
Bacterial Strains and Microbiological Culture Conditions

B dentium ATCC 27678 was cultured anaerobically in de Man, Rogosa and Sharpe (MRS) media (Difco, Franklin Lakes, NJ) or in a fully defined media, Lactic Acid Bacteria Defined Media 4 (LDM4).[43] *B ovatus* ATCC 8483 was cultured anaerobically in brain–heart–infusion broth (BHI) (Difco) supplemented with 2% yeast extract and 0.2% cysteine or in a Chemically Defined Minimal Media (CDMM).[43] All cultures were grown in an Anaerobe Systems (Morgan Hill, CA) AS-580 anaerobic chamber supplied with a mixture of 10% CO_2, 5% H_2, and 85% N_2. To heat-kill bacteria, *B dentium* was grown in MRS overnight, centrifuged at $5000 \times g$ for 10 minutes to pellet bacteria, and the pellet was washed 2 times with sterile phosphate-buffered saline (PBS). PBS suspensions were heated at $60°C$ for 30 minutes. Cell nonviability was confirmed by plating on MRS agar overnight anaerobically at $37°C$.

B dentium Conditioned Media and Negative Media Controls

For in vitro enteroid experiments, *B dentium* cultures were grown overnight in MRS. At the exponential phase these cultures were used to inoculate LDM4 (OD_{600nm} adjusted to 0.1) and incubated anaerobically at $37°C$ for 24 hours. In LDM4, *B dentium* reached OD_{600nm} of 1.87 ± 0.3, corresponding to approximately 4×10^8 colony-forming units (CFUs). The bacteria were centrifuged to remove cells ($5000 \times g$, 10 min) and the supernatant was adjusted to pH 7.0 by addition of NaOH. The pH-adjusted supernatant was filtered through a 0.2-μm membrane filter (Millipore, San Diego, CA). Cultures were filtered with a 3-kilodalton filter according to the manufacturer's instructions (Amicon Ultracel, 3 kilodaltons; Millipore) and lyophilized. Lyophilized supernatant was resuspended in mouse or human enteroid differentiation media to generate *B dentium*–conditioned media (CM). Uninoculated LDM4 bacterial media was treated using the same conditions to generate negative LDM4 media control. Enteroid culture media alone was used as negative media controls. To remove acetate from *B dentium* CM, we incubated acetyl-coenzyme A synthetase (A1765; Sigma, St. Louis, MO), 2 mmol/L coenzyme A (C3144-10MG; Sigma), 20 mmol/L adenosine triphosphate (A7699; Sigma), and 50 mmol/L $MgCl_2$ (M8266; Sigma) and incubated aerobically at $37°C$ for 3 hours. Loss of acetate was confirmed using an Acetate

Colorimetric Assay Kit (cat. MAK086; Sigma) according to the manufacturer's details.

Gnotobiotic Mouse Models and Intestinal Bacterial Colonization

Animal care and experimental procedures were approved by the Institutional Animal Care and Use Committee at Baylor College of Medicine (Houston, TX) in accordance with all guidelines set forth by the US National Institutes of Health (Baylor College of Medicine Institutional Animal Care and Use Committee approved protocol AN-6706). Germ-free Swiss Webster Mice were purchased from Taconic (Renssalaer, NY) and bred in the Gnotobiotic Animal Facility at Baylor College of Medicine to create an outbred colony of germ-free mice. Adult (age, 6–9 mo) male and female mice from this colony were maintained under germ-free or gnotobiotic conditions in separate flexible isolators fed with high-efficiency particulate–filtered air. Mice were kept under filter-top cages (3–5 mice per cage) with ad libitum access to irradiated food and water. Mice were provided with sterile Select Rodent 50 IF/6F auto 5V0F chow (cat. 3002875-703; Lab Diet.com, St. Louis, MO). To mono-associate germ-free mice, *B dentium* ATCC 27678 and *B ovatus* ATCC 8483 were grown in the culture conditions described earlier. Bacteria were harvested in log-phase growth and the OD_{600} of the culture was used to approximate cell viability based on previous growth curve data. Cell viability in the gavage mixture was verified by dilution plating on MRS or BHI agar immediately before the gavage procedure and was confirmed to be approximately 1.6×10^9 viable cells per milliliter. The cultures were prepared anaerobically and remained in anaerobic tubes until administered to the mice. Mice were oral-gavaged with 3.2×10^8 CFU/mL (in 0.2 mL) of live *B dentium* and 3.0×10^8 CFU/mL^{-1} (in 0.2 mL) of live *B ovatus*. For heat-killed treatment, mice received 3.2×10^8 CFU/mL^{-1} (in 0.2 mL) of heat-killed *B dentium* via oral gavage (as calculated from OD_{600}). Control mice received only sterile MRS broth. Mouse numbers were as follows: germ-free (MRS broth): males = 27, females = 30; live *B dentium* experiments: males n = 28, females n = 29; live *B ovatus*: males = 5, females = 5; and heat-killed *B dentium* males = 5, and females n = 5. Oral gavages were administered once every other day for 1 week with 1 supplemental gavage a week later (4 total treatments). Mono-association and germ-free status were monitored over the course of the experiment by plating individual fecal samples on MRS, BHI, and blood agar (Hardy Diagnostics, Santa Maria, CA). Plates were incubated at $37°C$ aerobically and anaerobically and examined for growth at 24 and 48 hours. The weight of each mouse was monitored upon exiting the isolators (on day 17), and mice were euthanized 72 hours after the last gavage. For behavior analysis, 20 SPF mice (males = 10, females = 10) mice were used in this study.

Mouse Intestinal Preparation

For tissue preparation, the small and large intestine carefully were removed immediately after euthanasia and dissected rapidly. Mouse terminal ileum (3–6 cm above the cecum) and mouse distal colon were cut into 2 sections. One segment was collected in TRIzol (Thermo Fisher, Waltham,

MA) for RNA extraction and gene expression analysis. The other segment was fixed in Carnoy's fixative, embedded with paraffin, and sectioned.

Fecal Matter Processing for Mass Spectral Analysis

Samples of fecal content (50–100 mg) were homogenized manually and suspended in 200 μL of 99% methanol on ice. The mixture was centrifuged at 21,130 $\times$ g for 2 minutes at 4°C. The supernatant (fecal water) was transferred into tubes containing 3-kilodalton filters and centrifuged at 14,000 $\times$ g for 30 minutes at room temperature. The filtrate (size, $\leq$3 kilodaltons) then was removed and stored at -80°C. Liquid chromatography with tandem mass spectrometry (LC-MS/MS) was used to quantify 5-HT concentrations from this preparation. For analysis of intestinal luminal content, 4 cm of terminal ileum and 4 cm of mid-colon were flushed by blunted syringe with 500 μL sterile PBS. The samples then were processed as described earlier for the fecal water preparation and stored at -80°C.

Quantification of Serotonin Concentration by LC-MS/MS

Chemicals and reagents. Serotonin hydrochloride, formic acid (FA), and heptafluorobutyric acid were obtained from Sigma Aldrich (St. Louis, MO). Serotonin-d4 hydrochloride was obtained from Santa Cruz Biotech (Dallas, TX). Optima LC/MS-grade water and acetonitrile (ACN) were obtained from Thermo-Fisher Scientific (Waltham, MA). Individual calibration standards were prepared at serotonin concentrations of 0.98, 3.9, 15.6, 62.5, 250, and 1000 ng/mL using an aqueous internal standard solution that contains 450 ng/mL of serotonin-d4 as the diluent.

Sample preparation. To prepare samples for LC-MS analysis, frozen samples were thawed and immediately vortexed for 1 minute. The samples then were centrifuged at 10,000 $\times$ g for 5 minutes. Ninety microliters of an aqueous internal standard solution containing 500 ng/mL of serotonin-d4 was added to a 10-μL volume of each sample and vortex-mixed for 15 seconds; the internal standard (IS) concentration was consistent between calibration standards and samples. Samples then were loaded into 0.5-mL autosampler vials and submitted for LC-MS/MS analysis.

Chromatography. Chromatography was performed on a Shimadzu (Kyoto, Japan) Nexera-XR high-performance liquid chromatography system consisting of an SIL-20ACxr autosampler, a CTO-20AC column oven, and 2 LC-20ADxr binary pumps. Sample (5 μL) was loaded onto a Phenomenex Luna C18(2) (150 $\times$ 1 mm, 3 μm, 100 Å pore) (Torrance, CA) reverse-phase column equipped with a Phenomenex Security Guard C18 (4 $\times$ 2 mm) guard column. The aqueous mobile phase A (phase A) consisted of H$_2$O:ACN:FA:heptafluorobutyric acid (99.3:0.5:0.1:0.1 v/v/v/v) and the organic mobile phase B (phase B) consisted of methanol:FA (99.9:0.1 v/v). The mobile phase flow rate was 100 μL/min. The elution gradient was optimized as follows: started from 5% phase B and increased to 60% phase B over 9 minutes; decreased from 60% phase B back to 5%

phase B over 0.1 minutes; and was maintained at 5% phase B for the duration of the 12-minute chromatographic run.

Mass spectrometry. Selected reaction monitoring was performed on a Sciex (Framingham, MA) 6500 QTRAP MS system with a Turbo V source and TurboIonSpray probe installed. The MS was operated in the positive ion mode under the following conditions: curtain gas: 20 psi; collision gas: high; spray voltage: + 5 kV; ion source gas 1: 25 psi; ion source gas 2: 25 psi; interface heater temperature: 200°C; Q1 and Q3 resolution: unit/unit; dwell time: 220 ms; declustering potential (DP): +20 V; entrance potential (EP): +8 V; and collision exit potential (CXP): +10 V. The instrument was calibrated using Sciex PPG calibration standard and tuned to the manufacturer's specifications. Selected-reaction monitoring (SRM) transitions monitored for serotonin were 177.1 $\rightarrow$ 160.1 (collision energy [CE]: +17 electron volts [eV]) and 177.1 $\rightarrow$ 115.1 (CE: +38 eV). For serotonin-d4, the SRM transitions 181.1 $\rightarrow$ 164.1 (CE: +17 eV) and 181.1 $\rightarrow$ 119.1 (CE: +38 eV) were monitored. Data were acquired with Analyst Software (SCIEX, Framingham, MA, version 1.6.2) and quantification was performed using Multiquant Software (SCIEX version 3.0.1).

Quantification of SCFA Concentration by LC-MS/MS

Chemicals and reagents. Optima LC/MS-grade ACN, FA, methanol, and water were obtained from Thermo-Fisher Scientific. Authentic SCFA reference materials (acetic acid, propionic acid, butyric acid, isobutyric acid, pentanoic acid, isopentanoic acid, and 2-methylbutyric acid) were obtained from Millipore-Sigma (Burlington, MA). Reagents used in the derivatization of the SCFAs include aniline and [13C6]-aniline (for carbon-13 labeled IS preparations) and were obtained from Millipore-Sigma, and 1-(3-dimethylaminopropyl)-3-ethylcarbodiimide hydrochloride, 2-mercaptoethanol, and succinic acid were obtained from Thermo-Fisher Scientific. Derivatization reactions for the preparation of the analytes (N-phenyl-SCFA derivatives) and corresponding IS (N- [(^{13}C$_6$)-phenyl]-SCFA derivatives) were performed as previously described.[44] Individual calibration standards were prepared at N-phenyl SCFA derivative concentrations of 9.8, 39.0, 156, 625, 2500, and 10,000 nmol/L using an internal standard solution that contains 2250 nmol/L of [^{13}C$_6$]-phenyl-SCFA derivatives as the diluent.

Sample derivatization procedures. Overnight anaerobic cultures of *B dentium* in LDM4 media and *B ovatus* in CDMM media were used for SCFA analysis. Before sample derivatization, each filter-sterilized media sample was diluted 2-fold in ACN. The SCFA-derivatization reaction for each media sample was performed by mixing a 10-μL volume of the diluted media sample, a 100-μL volume of a 100-mmol/L aniline solution, and a 50-μL volume of a 100 mmol/L 1-(3-dimethylaminopropyl)-3-ethylcarbodiimide hydrochloride solution. Each sample mixture then was vortex-mixed for 20 seconds, incubated at +4°C for 2 hours, and then quenched by the addition of 50-μL volumes of a 100-mmol/L mercaptoethanol solution and a 250-mmol/L succinic acid

solution followed by an additional 2 hour incubation at $+4°C$. After quenching, a 10-μL volume of the derivatized media sample was diluted in a 90-μL volume of an IS solution that contained 2500 nmol/L of $[^{13}C_6]$-phenyl-SCFA derivatives as the diluent—the IS concentration was consistent between calibration standards and samples.

Fecal content from germ-free, *B dentium* mono-associated, and *B ovatus* mono-associated mice was stored at -80°C until analysis. The wet weight of fecal material was determined gravimetrically, and an appropriate volume of an ice-cold 1:1 ACN:water solution was added to each sample to obtain a normalized fecal material density of 0.1 mg/μL of solvent. The SCFA-derivatization reaction for each fecal sample was performed by mixing an 85-μL volume of the sample extract, a 10-μL volume of a 100-mmol/L aniline solution, and a 5-μL volume of a 100-mmol/L 1-(3-dimethylaminopropyl)-3-ethylcarbodiimide hydrochloride solution. Each sample mixture then was vortex-mixed for 20 seconds, incubated at $+4°C$ for 2 hours, and then quenched by the addition of a 6.0-μL volume of a 100 mmol/L mercaptoethanol solution, a 9.4-μL volume of a 250-mmol/L succinic acid solution, and 14.6 μL of water followed by an additional 2 hour incubation at $+4°C$. After quenching, the derivatized fecal samples were diluted 10-fold in a 20:80 acetonitrile:water solution, and then diluted further by the addition of a 10-μL volume of the diluted derivatized fecal sample in a 90-μL volume of an IS solution that contained 2500 nmol/L of ($[^{13}C_6]$-N-phenyl-SCFA) derivatives as the diluent—the IS concentration was consistent between calibration standards and samples..

Chromatography. Chromatography was performed using the same high-performance liquid chromatography system as described for the serotonin measurements earlier. A derivatized sample (5 μL) was loaded onto a Restek Viva BiPh Biphenyl (150 × 1 mm, 5 μm, 300 Å pore) (Bellefonte, PA) reverse-phase column equipped with a Restek Viva BiPh Biphenyl (10 × 2.11 mm, 5 μm) guard column. The aqueous mobile phase (phase A) consisted of water:FA (99.9:0.1 v/v) and the organic mobile phase (phase B) consisted of ACN:FA (99.9:0.1 v/v). The mobile phase flow rate was 200 μL/min. The elution gradient was optimized as follows: held at 5% B for 2 minutes; increased from 5% B to 50% B over 7 minutes; reduced from 50% B to 5% B over 0.1 minutes; and maintained at 5% B for the duration of the 12-minute chromatographic run.

Mass spectrometry. SRM scanning was performed using the same MS system described earlier. The MS was operated in the positive ion mode under the following conditions: curtain gas: 20 psi; collision gas: high; spray voltage: + 5 kV; ion source gas 1: 25 psi; ion source gas 2: 25 psi; interface heater temperature: 200°C; Q1 and Q3 resolution: unit/unit; dwell time: 20 ms; and CXP: +10 V. The instrument was calibrated using the Sciex PPG calibration standard and tuned to the manufacturer's specifications. The molecule-specific LC-MS/MS parameters for all of the N-phenyl-SCFA and ($[^{13}C_6]$-N-phenyl-SCFA) derivatives are listed in Table 1.

Mouse and Human Enteroid Cultures

To create mouse intestinal enteroids, Swiss Webster mice were anesthetized with isoflurane before euthanization by cervical dislocation. Tissues were dissected rapidly and enteroids were generated as previously described.[45] Briefly, a 5-cm length of terminal ileum (<10 cm proximal to the cecum) was excised, washed with ice-cold PBS (Gibco, Gaithersburg, MD), and opened longitudinally. The ileum then was cut into approximately 1-cm length pieces and placed in a 15-mL conical tube containing 5 mL of ice-cold PBS and 3 mmol/L EDTA (Gibco). The tubes were incubated at 4°C rocking for 30 minutes. Crypts were disrupted mechanically by shaking in 5 mL of ice-cold PBS with D-sorbitol and sucrose and collected after filtering through a 70-μm cell strainer (cat. 431751; Corning, Corning, NY). Crypts were centrifuged, resuspended in Matrigel (Corning), and incubated with IntestiCult Organoid Growth media (cat. 06005; StemCell Technologies, Vancouver, Canada) containing 2% penicillin-streptomycin (Life Technologies, Carlsbad, CA). All enteroids were passaged more than 2 times to ensure no tissue fragments remained. Enteroids were differentiated by adding media without Wnt and incubated at 37°C with 5% CO_2 for 5 days before use.

HIEs were generated from adult jejunum by the Texas Medical Center Digestive Diseases Center Gastrointestinal Experimental Model Systems (GEMS) Core at Baylor College of Medicine, as previously described.[46–48] Established HIE cultures from patient J2 were used. Complete HIE media without growth factors, with growth factors, and differentiation media were prepared as previously described.[46,49] In addition to the established J2 HIE line, tetracycline-inducible (tet)-Neurogenin-3 (NGN3)-expressing HIEs were created using lentivirus transduction as previously described.[46] All HIEs were grown as 3-dimensional (3D) cultures and as flat 2-dimensional (2D) monolayers on 96-well plates as described in a previously published protocol.[49–56] *tet*NGN3 HIEs were treated with 1 μg/mL doxycycline for 4 days in differentiation media to induce *NGN3* expression and drive enteroendocrine cell fate.

Differentiated normal HIEs, tet*NGN3* HIEs, and mouse enteroids grown in 3 dimensions were microinjected as previously described[45] using a Nanoject microinjector (Drummon Scientific Company, Broomall, PA) with an injection volume of 16.5 nL. Enteroids were injected with either enteroid media (negative culture media control), uninoculated LDM4 media (in enteroid media), *B dentium*–CM (in enteroid media), or 5 mmol/L sodium acetate (cat. S5636; Sigma-Aldrich) in enteroid media. As negative controls, enteroids also were microinjected with 1 μg/mL lipopolysaccharide (LPS) (derived from *E coli* O111:B4, tlrl-3pelps; InvivoGen, San Diego, CA) or heat-killed *B dentium*. For 2D HIE and *tet*NGN3 HIE monolayers, treatments were added apically to wells. All enteroids (mouse and human being) were incubated overnight for 16 hours. Supernatant from each well was collected to quantify 5-HT concentrations via LC-MS/MS. In addition, enteroids from each treatment also were fixed in 4% paraformaldehyde and embedded in paraffin for staining.

Human Intestinal Epithelial Cell Culture

To confirm the adherence of *B dentium* to intestinal mucus, the mucus-secreting human colon LS174T cells ATCC CL-188 were seeded at a density of 1×10^5 cells onto Corning Costar 24-well cell culture plates containing poly-D-lysine–coated coverslips. Confluent coverslips were inoculated with 2×10^5 viable *B dentium* cells, and then incubated anaerobically at 37°C for 1 hour. After the incubation period, the coverslips were washed thoroughly with PBS ($3\times$) and processed for scanning electron microscopy.

Scanning Electron Microscopy

After incubation with bacteria, washed coverslips were fixed in 2.5% glutaraldehyde in PBS for 1 hour at room temperature. Alternatively, intestinal segments were opened lengthwise, thoroughly washed with PBS, and fixed in 2.5% glutaraldehyde in PBS for 4 hours at room temperature. Cells then were incubated with 1% osmium tetroxide in PBS (cat. 201030; Sigma-Aldrich) overnight at 4°C. Tissue and coverslips were dehydrated with ethanol (10 minutes each in 25%, 50%, 75%, 80%, 95%, and 4

cycles of 100%) at room temperature. In a desktop sputtering system (Denton Desk II), cells were coated with 20 nm of gold and viewed via scanning electron microscopy (FEI XL-30FEG) at 12 kV as previously described.[57] Adobe Photoshop (San Jose, CA) was used to falsely color resulting images based on the morphology of bacterial cells.

Intestinal Tissue Staining

Immunofluorescence. Staining was performed on 7-μm, paraffin-embedded sections of mouse intestine or enteroids. After dehydration, slides were incubated in Antigen Unmasking Solution Citrate Buffer pH 6 (Vector Labs, Burlingame, CA) for 20 minutes at 100°C in a steamer for antigen retrieval, then blocked for 1 hour at room temperature in 10% donkey serum. Staining was performed with primary antibodies (Table 2) overnight at 4°C. Primary antibodies were recognized by the following secondary antibodies (Table 2) diluted at 1:1000 in PBS-tween (PBS-T) and incubated for 1 hour at room temperature. Nuclei were stained with Hoechst 33342 (Invitrogen) for 10 minutes at room temperature and all slides were cover-slipped with

Table 1. LC-MS/MS Transitions and Molecule-Specific Parameters for Selected Reaction Monitoring of the N-Phenyl Derivatives of SCFAs and their Carbon-13–Labeled Internal Standard Compounds

Q1, m/z	Q3, m/z	Time, mS	ID	CE, eV	DP, V	EP, V	CXP, V
136.1	94	20	N-phenyl acetamide 136>94	+22	+60	+9	+15
136.1	77	20	N-phenyl acetamide 136>77	+40	+60	+9	+15
142.1	100	20	$^{13}C_6$-N-phenyl acetamide 136>100	+22	+60	+10	+15
142.1	84	20	$^{13}C_6$-N-phenyl acetamide 136>84	+51	+60	+10	+15
150.1	94	20	N-phenyl propanamide 150>94	+22	+70	+9	+15
150.1	77	20	N-phenyl propanamide 150>77	+42	+70	+9	+15
156.1	100	20	$^{13}C_6$-N-phenyl propanamide 156>100	+26	+60	+10	+15
156.1	82.9	20	$^{13}C_6$-N-phenyl propanamide 156>82.9	+45	+60	+10	+15
164.1	94	20	N-phenyl butanamide 164>94	+23	+75	+9	+15
164.1	77	20	N-phenyl butanamide 164>77	+45	+75	+9	+15
170.1	100	20	$^{13}C_6$-N-phenyl butanamide 170>100	+25	+60	+10	+15
170.1	82.9	20	$^{13}C_6$-N-phenyl butanamide 170>82.9	+49	+60	+10	+15
164.1	94	20	N-phenyl isobutanamide 164>94	+24	+72	+9	+15
164.1	77	20	N-phenyl isobutanamide 164>77	+46	+72	+9	+15
170.1	100	20	$^{13}C_6$-N-phenyl isobutanamide 170>100	+24	+72	+9	+15
170.1	82.9	20	$^{13}C_6$-N-phenyl isobutanamide 170>82.9	+46	+72	+9	+15
178.1	94	20	N-phenyl pentanamide 178>94	+23	+80	+9	+15
178.1	77	20	N-phenyl pentanamide 178>77	+48	+80	+9	+15
184.1	100	20	$^{13}C_6$-N-phenyl pentanamide 184>100	+23	+80	+9	+15
184.1	82.9	20	$^{13}C_6$-N-phenyl pentanamide 184>82.9	+48	+80	+9	+15
178.1	94	20	N-phenyl isopentanamide 178>94	+22	+80	+9	+15
178.1	77	20	N-phenyl isopentanamide 178>77	+48	+80	+9	+15
184.1	100	20	$^{13}C_6$-N-phenyl isopentanamide 184>100	+22	+80	+9	+15
184.1	82.9	20	$^{13}C_6$-N-phenyl isopentanamide 184>82.9	+48	+80	+9	+15
178.1	94	20	N-phenyl 2-methylbutanamide 178>94	+23	+80	+9	+15
178.1	77	20	N-phenyl 2-methylbutanamide 178>77	+49	+80	+9	+15
184.1	100	20	$^{13}C_6$-N-phenyl 2-methylbutanamide 184>100	+23	+80	+9	+15
184.1	82.9	20	$^{13}C_6$-N-phenyl 2-methylbutanamide 184>82.9	+49	+80	+9	+15

CD, charged detection; CE, collision energy; CXP, collision-cell exit potential; EP, entrance potential; eV, electron volt; V, volts.

Table 2. Primary and Secondary Antibodies

Type	Target	Species	Recognizes	Company	Category	Dilution
Primary	ChgA	Rabbit	Human	Novus Biologicals, Littleton, CO	NBP2-53140	1:200
Primary	ChgA	Rabbit	Mouse	Abcam, Cambridge, MA	ab45179	1:200
Primary	5-HT	Goat	Mouse, human	Immunostar, Hudson, WI	20079	1:100
Primary	5-HT	Rat	Mouse	Santa Cruz	sc-58031	1:100
Primary	SERT	Rabbit	Mouse, human	Immunostar	24330	1:5000
Primary	FFAR2	Rabbit	Mouse	Millipore, Burlington, MA	ABC299	1:200
Primary	CHAT	Goat	Mouse, human	Millipore	AB144P	1:100
Secondary	Anti-goat Alexa Fluor 488	Donkey	Goat	Life Technologies	A11055	1:1000
Secondary	Anti-goat Alexa Fluor 555	Donkey	Goat	Life Technologies	A-21432	1:1000
Secondary	Anti-rabbit Alexa Fluor 488	Donkey	Rabbit	Life Technologies	R37116	1:1000
Secondary	Anti-rabbit Alexa Fluor 555	Donkey	Rabbit	Life Technologies	A31572	1:1000

mounting media (Life Technologies) and imaged using a Nikon Eclipse 90i epifluorescence microscope (Nikon, Tokyo, Japan).

Tissue Gram stain. To examine bacterial colonization within the mucus layer, Gram staining was performed on intestinal tissue sections. Briefly, paraffin-embedded tissue sections were dehydrated, and then incubated with crystal violet followed by gram iodine as a mordant. After exposure to a decolorizer, solvent sections were stained with gram safranin, followed by picric acid–acetone. After subsequent dehydration through a series of alcohols and xylene, sections were cover-slipped and imaged via brightfield microscopy.

Fluorescence in situ hybridization staining. Carnoy's fixed, paraffin-embedded, mouse intestinal tissue sections (4-μm–thick sections) were mounted on glass slides. Briefly, sections were dehydrated in ethanol and incubated with the probe in a humidifying dark chamber at 45°C. The probe used was a previously validated, 5' Texas Red–labeled *Bifidobacterium* genus–specific probe (Bif164; 5'-CATCCGGCATTAC-CACCC-3') (Integrated DNA Technologies, Coralville, IA) targeted to the 164–181 bp region of 16S ribosomal RNA.[58] The probe was hybridized to the samples by adding 15 μL of probe (2 μmol/L) to each slide and placing in a 45°C hybridization chamber for 45 minutes. Nuclei were labeled with 4',6-diamidino-2-phenylindole. Images were acquired using a Nikon Eclipse 90i epifluorescence microscope as previously described.[45,59,60]

Microscopy. Fluorescence and transmitted light images were taken on an upright Nikon Eclipse 90i microscope using Nikon Elements software for image acquisition and processing. The following objectives were used: 20× Plan Apochromat Objective (numerical aperture, 0.75) differential interference contrast objective and 40× Plan Apochromat Objective (numerical aperture, 0.95) differential interference contrast objective. Fluorescence images were recorded using a Cool-SNAP HQ2 camera (Photometrics, Tucson, AZ) with a SPECTRA X LED light source (Lumencor, Beaverton, OR). Color images for H&E sections were recorded using a DS-Fi1-U2 camera (Nikon, Tokyo, Japan).

Quantitative Real-Time Polymerase Chain Reaction

To quantify relative messenger RNA (mRNA) expression of each gene of interest, total RNA was extracted from ileum and colon samples stored in TRIzol according to the manufacturer's instructions. Complementary DNA (cDNA) was generated from 1 μg RNA via the SensiFAST cDNA synthesis kit (Bioline USA, Inc, Taunton, MA). Alternatively, genomic DNA was isolated from fecal extracts using the Zymo genomic DNA MiniPrep Kit (cat. 11-317C; Zymo Research, Irvine, CA) with the addition of bead beating. Quantitative real-time PCR (qPCR) was performed using a QuantStudio 3 (Applied Biosystems, Foster City, CA) qPCR machine. Forward and reverse primers specific for each gene (Table 3) were added to FastSYBR Green mastermix (Thermo-Fisher Scientific) and cDNA. Primers were obtained from ABI Primer 3 software, PrimerBank, or from previous literature.[25,61–64] Target genes were normalized to the housekeeping gene glyceraldehyde-3-phosphate dehydrogenase and relative expression was calculated using the Delta-Delta-Ct (ddCT) method.

Brain RNA In Situ Hybridization

Brains of adult germ-free and *B dentium* mono-associated mice (n = 5–6 per group) were dissected rapidly, cut along the sagittal midline, and placed in molds with tissue freezing media (O.C.T., TissueTek, Sakura, Torrance, CA) for frozen sectioning. RNA in situ hybridization (ISH) was performed on 25-μm–thick sagittal sections. Digoxigenin-labeled mRNA antisense probes were generated against *htr2a* using reverse-transcribed mouse cDNA as a template and a RNA digoxigenin-labeling kit from Roche (Basel, Switzerland). Primer sequences for the *htr2a* probe are as follows: forward: GCGATTTAGGTGACACTA-TAGCCTAATGACTTCAACTCCAGGG; reverse: GCGTAA-TACGACTCACTATAGGGCCACAAAAGAGCCTATGAGGAC. ISH was performed by the RNA in situ Hybridization Core at Baylor College of Medicine using an automated robotic platform. Quantitative analysis of the fluorescence in situ

Table 3. Primers Used in This Study

Gene	Forward (5') sequence	Reverse (3') sequence	Reference
B dentium	ATCCCGGGGGTTCGCCT	GAAGGGCTTGCTCCCGA	Matsuki
B ovatus	AAGTCGAGGGGC AGCATT TT	CACAACTGACTTAACAATCC	Miyamoto
GAPDH	CATGGCCTTCCGTGTTCCTA	CCTGCTTCACCACCTTCTTGAT	61
CHGA	CCCACTGCAGCATCCAGTT	AGTCCCGACTGACCATCATCTTTC	25
TPH1	AAGAAATTGGCCTGGCTTC	GTTTGCACAGCCCAAACTC	25
FFAR2	ATCCTCCTGCTTAATCTGACCC	CGCACACGATCTTTGGTAGGT	Primerbank
SERT	TGGGCGCTCTACTACCTCAT	ATGTTGTCCTGGGCGAAGTA	60
Htr1a	TACTGGGCAATCACCGACCCTAT	GAGATGAGAAAGCCAATGAGCCAA	Primer 3
Htr1b	CCTGGTGATGCCTATCTGTAAGGA	AGTTTGTGGAACGCTTGTTTGAAGT	Primer 3
Htr1d	CCGAGAAAGGAAAGCCACTAAGAC	ATACTACAAAGAAAGGCAACCAGCA	Primer 3
htr1f	GACAACCACCATCAACTCCCTC	AAATCTGTAACTGCCAAGGAACAAA	Primer 3
Htr2a	ACATCCAGGTAAATCCAGACG	GATGTCACTTGCCATAGCTGA	Primer 3
Htr2c	AGAAGGGTGATGAGGAAGAGAACG	ACACAAAGAATACAATGCCAAGGACT	Primer 3
Htr3a	GCCACCCAGGAGGATACCAC	GCTCCCACTCGCCCTGATT	64
Htr4	TCGGCATAGTTGATGTGATAGAGAAA	ATGAGGAGAAACGGGATGTAGAAGG	Primer 3
Htr5a	AAAGTCAGGACTAGCACTCG	AAAGTCAGGACTAGCACTCG	64
Htr5b	CCCTTGATTTACACTGCC	CAGAAATGGAGCACAATTCAC	64
Htr6	CTGATGGTGGGATTGGTGGTGATG	GATGAGGCAGAGGTTGAGAATGGAG	Primer 3
Htr7	TTCGAGACTGCTCAAACAC	TGCAGCAGAGAGCTTCCGGT	64

hybridization (FISH) signal on sections was performed using software developed for the core by Dr James Carson as previously described.[65] Single-cell expression of *htr2a* within specific brain regions (manually defined in software) were categorized as weak, media, or strongly expressing based on the staining intensity for each region of the hippocampus separately. Four sagittal sections were analyzed per mouse, with 5–6 mice per treatment group.

Behavioral Testing: Marble Burying Test

This test was performed as previously described with slight modifications.[66–68] Mice were removed from gnotobiotic isolators and allowed to acclimate to the testing room without being disturbed for 1 hour before testing. Lighting conditions and noise levels were kept constant across all tests. Clean transparent polycarbonate boxes (30 × 30 cm) were filled with a 5-cm layer of fresh, unscented, wood chip bedding. Twenty-five black glass marbles were placed lightly on top of the bedding, spaced equidistantly (5-cm apart) in a 5 × 5 arrangement. Animals (n = 12–13 mice per group) were placed gently in the corner of the testing cage and left undisturbed for 13 minutes, with the researcher out of the room. At the end of the test the mouse was removed promptly, with care taken to not disturb the marbles. The number of marbles buried during the test was recorded by 2 independent blinded observers. Marbles were considered buried when >60% was covered by bedding material. Scores from each observer for each mouse were averaged, and are presented as the percentage buried (number buried/total number of marbles in the cage). Marbles were rinsed in 70% ethanol, then in water, and dried before the next test. Bedding in the cage was flattened using a sterile cage bottom between tests. Cage bedding was changed between sexes and between groups of different colonization status.

Footprint Analysis

The commonly used footprint analysis was used to analyze motor coordination by assessing gait during normal walking.[69,70] Briefly, hind paws were painted with blue ink and mice were encouraged to walk through a narrow, enclosed corridor in a straight line over paper by the presence of bedding, food, and darkness at the end of the tunnel. The footprint test was repeated until at least 2 clear sets of footprints were obtained per mouse (n = 5–7 mice/ group). The distance was measured from the center of footpad for each metric (sway, stance, and stride) and was averaged from 2–3 runs per mouse.

Balance Beam

The balance beam test was used to detect subtle deficits in motor skills and balance.[70,71] Each mouse was placed on a brightly lit platform and allowed to transverse a narrow beam to reach an enclosed safety box at the end of the beam. Mice were trained before tests with 3 successful training runs. The time to cross the beam was defined as 2 successful trials in which the mouse did not stall on the beam. The times to complete crossing the beam were recorded and averaged per mouse. This procedure was videorecorded to allow for finer analysis of paw slipping (n = 5–7 mice/group).

Statistical Analysis

Biostatistical analyses were performed using GraphPad Prism (version 6) software (GraphPad, Inc, La Jolla, CA).

Comparisons were made with either 1-way or 2-way analysis of variance and the Bonferroni post hoc test. Nonparametric data were log-transformed to pass normality tests before analysis by analysis of variance. Differences between the groups were considered significant at $P < .05$ (*) and the data are presented as means ± SEM.

References

1. Ley RE, Peterson DA, Gordon JI. Ecological and evolutionary forces shaping microbial diversity in the human intestine. Cell 2006;124:837–848.

2. O'Hara JR, Skinn AC, MacNaughton WK, Sherman PM, Sharkey KA. Consequences of Citrobacter rodentium infection on enteroendocrine cells and the enteric nervous system in the mouse colon. Cell Microbiol 2006; 8:646–660.

3. Qin J, Li R, Raes J, Arumugam M, Burgdorf KS, Manichanh C, Nielsen T, Pons N, Levenez F, Yamada T, Mende DR, Li J, Xu J, Li S, Li D, Cao J, Wang B, Liang H, Zheng H, Xie Y, Tap J, Lepage P, Bertalan M, Batto JM, Hansen T, Le Paslier D, Linneberg A, Nielsen HB, Pelletier E, Renault P, Sicheritz-Ponten T, Turner K, Zhu H, Yu C, Li S, Jian M, Zhou Y, Li Y, Zhang X, Li S, Qin N, Yang H, Wang J, Brunak S, Dore J, Guarner F, Kristiansen K, Pedersen O, Parkhill J, Weissenbach J, MetaHIT Consortium, Bork P, Ehrlich SD, Wang J. A human gut microbial gene catalogue established by metagenomic sequencing. Nature 2010;464: 59–65.

4. Gershon MD. 5-Hydroxytryptamine (serotonin) in the gastrointestinal tract. Curr Opin Endocrinol Diabetes Obes 2013;20:14–21.

5. Resnick RH, Gray SJ. Distribution of serotonin (5-hydroxytryptamine) in the human gastrointestinal tract. Gastroenterology 1961;41:119–121.

6. Gershon MD. Review article: roles played by 5-hydroxytryptamine in the physiology of the bowel. Aliment Pharmacol Ther 1999;13(Suppl 2):15–30.

7. Erspamer V. Occurrence of indolealkylamines in nature. New York: Springer-Verlag, 1966.

8. Kim JJ, Khan WI. 5-HT7 receptor signaling: improved therapeutic strategy in gut disorders. Front Behav Neurosci 2014;8:396.

9. Bertrand PP, Barajas-Espinosa A, Neshat S, Bertrand RL, Lomax AE. Analysis of real-time serotonin (5-HT) availability during experimental colitis in mouse. Am J Physiol Gastrointest Liver Physiol 2010; 298:G446–G455.

10. Gershon MD, Tack J. The serotonin signaling system: from basic understanding to drug development for functional GI disorders. Gastroenterology 2007;132:397–414.

11. Hoffman JM, Tyler K, MacEachern SJ, Balemba OB, Johnson AC, Brooks EM, Zhao H, Swain GM, Moses PL, Galligan JJ, Sharkey KA, Greenwood-Van Meerveld B, Mawe GM. Activation of colonic mucosal 5-HT(4) receptors accelerates propulsive motility and inhibits visceral hypersensitivity. Gastroenterology 2012; 142:844–854 e4.

12. Mawe GM, Hoffman JM. Serotonin signalling in the gut—functions, dysfunctions and therapeutic targets. Nat Rev Gastroenterol Hepatol 2013;10:473–486.

13. Baganz NL, Blakely RD. A dialogue between the immune system and brain, spoken in the language of serotonin. ACS Chem Neurosci 2013;4:48–63.

14. Clarke G, Grenham S, Scully P, Fitzgerald P, Moloney RD, Shanahan F, Dinan TG, Cryan JF. The microbiome-gut-brain axis during early life regulates the hippocampal serotonergic system in a sex-dependent manner. Mol Psychiatry 2013;18:666–673.

15. Winstanley CA, Theobald DE, Dalley JW, Glennon JC, Robbins TW. 5-HT2A and 5-HT2C receptor antagonists have opposing effects on a measure of impulsivity: interactions with global 5-HT depletion. Psychopharmacology (Berl) 2004;176:376–385.

16. Cools R, Roberts AC, Robbins TW. Serotoninergic regulation of emotional and behavioural control processes. Trends Cogn Sci 2008;12:31–40.

17. Wikoff WR, Anfora AT, Liu J, Schultz PG, Lesley SA, Peters EC, Siuzdak G. Metabolomics analysis reveals large effects of gut microflora on mammalian blood metabolites. Proc Natl Acad Sci U S A 2009; 106:3698–3703.

18. Yano JM, Yu K, Donaldson GP, Shastri GG, Ann P, Ma L, Nagler CR, Ismagilov RF, Mazmanian SK, Hsiao EY. Indigenous bacteria from the gut microbiota regulate host serotonin biosynthesis. Cell 2015;161:264–276.

19. Sjogren K, Engdahl C, Henning P, Lerner UH, Tremaroli V, Lagerquist MK, Backhed F, Ohlsson C. The gut microbiota regulates bone mass in mice. J Bone Miner Res 2012;27:1357–1367.

20. Hata T, Asano Y, Yoshihara K, Kimura-Todani T, Miyata N, Zhang XT, Takakura S, Aiba Y, Koga Y, Sudo N. Regulation of gut luminal serotonin by commensal microbiota in mice. PLoS One 2017;12:e0180745.

21. Desbonnet L, Garrett L, Clarke G, Bienenstock J, Dinan TG. The probiotic Bifidobacteria infantis: an assessment of potential antidepressant properties in the rat. J Psychiatr Res 2008;43:164–174.

22. Diaz Heijtz R, Wang S, Anuar F, Qian Y, Bjorkholm B, Samuelsson A, Hibberd ML, Forssberg H, Pettersson S. Normal gut microbiota modulates brain development and behavior. Proc Natl Acad Sci U S A 2011; 108:3047–3052.

23. Luczynski P, McVey Neufeld KA, Oriach CS, Clarke G, Dinan TG, Cryan JF. Growing up in a bubble: using germ-free animals to assess the influence of the gut microbiota on brain and behavior. Int J Neuropsychopharmacol 2016;19:pyw020.

24. Luk B, Veeraragavan S, Engevik M, Balderas M, Major A, Runge J, Luna RA, Versalovic J. Postnatal colonization with human "infant-type" Bifidobacterium species alters behavior of adult gnotobiotic mice. PLoS One 2018;13: e0196510.

25. Reigstad CS, Salmonson CE, Rainey JF 3rd, Szurszewski JH, Linden DR, Sonnenburg JL, Farrugia G, Kashyap PC. Gut microbes promote colonic serotonin production through an effect of short-

chain fatty acids on enterochromaffin cells. FASEB J 2015;29:1395–1403.

26. Brown AJ, Goldsworthy SM, Barnes AA, Eilert MM, Tcheang L, Daniels D, Muir AI, Wigglesworth MJ, Kinghorn I, Fraser NJ, Pike NB, Strum JC, Steplewski KM, Murdock PR, Holder JC, Marshall FH, Szekeres PG, Wilson S, Ignar DM, Foord SM, Wise A, Dowell SJ. The Orphan G protein-coupled receptors GPR41 and GPR43 are activated by propionate and other short chain carboxylic acids. J Biol Chem 2003; 278:11312–11319.

27. Karaki S, Mitsui R, Hayashi H, Kato I, Sugiya H, Iwanaga T, Furness JB, Kuwahara A. Short-chain fatty acid receptor, GPR43, is expressed by enteroendocrine cells and mucosal mast cells in rat intestine. Cell Tissue Res 2006;324:353–360.

28. Karaki S, Tazoe H, Hayashi H, Kashiwabara H, Tooyama K, Suzuki Y, Kuwahara A. Expression of the short-chain fatty acid receptor, GPR43, in the human colon. J Mol Histol 2008;39:135–142.

29. Tazoe H, Otomo Y, Kaji I, Tanaka R, Karaki SI, Kuwahara A. Roles of short-chain fatty acids receptors, GPR41 and GPR43 on colonic functions. J Physiol Pharmacol 2008;59(Suppl 2):251–262.

30. Nohr MK, Pedersen MH, Gille A, Egerod KL, Engelstoft MS, Husted AS, Sichlau RM, Grunddal KV, Poulsen SS, Han S, Jones RM, Offermanns S, Schwartz TW. GPR41/FFAR3 and GPR43/FFAR2 as cosensors for short-chain fatty acids in enteroendocrine cells vs FFAR3 in enteric neurons and FFAR2 in enteric leukocytes. Endocrinology 2013;154:3552–3564.

31. Martin AM, Lumsden AL, Young RL, Jessup CF, Spencer NJ, Keating DJ. The nutrient-sensing repertoires of mouse enterochromaffin cells differ between duodenum and colon. Neurogastroenterol Motil 2017; 29.

32. Akiba Y, Inoue T, Kaji I, Higashiyama M, Narimatsu K, Iwamoto K, Watanabe M, Guth PH, Engel E, Kuwahara A, Kaunitz JD. Short-chain fatty acid sensing in rat duodenum. J Physiol 2015;593:585–599.

33. Maruta K, Akiba Y, Kaji I, Kaunitz JD. Serotonin released by FFA2 activation stimulates HCO3- secretion, but induces mucosal injury in rat duodenum. Gastroenterology 2017;152:S13–S14.

34. Lin HV, Frassetto A, Kowalik EJ Jr, Nawrocki AR, Lu MM, Kosinski JR, Hubert JA, Szeto D, Yao X, Forrest G, Marsh DJ. Butyrate and propionate protect against diet-induced obesity and regulate gut hormones via free fatty acid receptor 3-independent mechanisms. PLoS One 2012;7:e35240.

35. Le Poul E, Loison C, Struyf S, Springael JY, Lannoy V, Decobecq ME, Brezillon S, Dupriez V, Vassart G, Van Damme J, Parmentier M, Detheux M. Functional characterization of human receptors for short chain fatty acids and their role in polymorphonuclear cell activation. J Biol Chem 2003;278:25481–25489.

36. Tsuruta T, Saito S, Osaki Y, Hamada A, Aoki-Yoshida A, Sonoyama K. Organoids as an ex vivo model for studying the serotonin system in the murine small

37. O'Callaghan A, van Sinderen D. Bifidobacteria and their role as members of the human gut microbiota. Front Microbiol 2016;7:925.

38. Fukuda S, Toh H, Hase K, Oshima K, Nakanishi Y, Yoshimura K, Tobe T, Clarke JM, Topping DL, Suzuki T, Taylor TD, Itoh K, Kikuchi J, Morita H, Hattori M, Ohno H. Bifidobacteria can protect from enteropathogenic infection through production of acetate. Nature 2011; 469:543–547.

39. Fukuda S, Toh H, Taylor TD, Ohno H, Hattori M. Acetate-producing bifidobacteria protect the host from enteropathogenic infection via carbohydrate transporters. Gut Microbes 2012;3:449–454.

40. Falony G, Vlachou A, Verbrugghe K, De Vuyst L. Cross-feeding between Bifidobacterium longum BB536 and acetate-converting, butyrate-producing colon bacteria during growth on oligofructose. Appl Environ Microbiol 2006;72:7835–7841.

41. Human Microbiome Project Consortium. Structure, function and diversity of the healthy human microbiome. Nature 2012;486:207–214.

42. Pokusaeva K, Johnson C, Luk B, Uribe G, Fu Y, Oezguen N, Matsunami RK, Lugo M, Major A, Mori-Akiyama Y, Hollister EB, Dann SM, Shi XZ, Engler DA, Savidge T, Versalovic J. GABA-producing Bifidobacterium dentium modulates visceral sensitivity in the intestine. Neurogastroenterol Motil 2017;29:e12904.

43. Engevik MA, Morra CN, Roth D, Engevik K, Spinler JK, Devaraj S, Crawford SE, Estes MK, Kalkum M, Versalovic J. Microbial metabolic capacity for intestinal folate production and modulation of host folate receptors. Front Microbiol 2019;10:2305.

44. Chan JC, Kioh DY, Yap GC, Lee BW, Chan EC. A novel LCMSMS method for quantitative measurement of short-chain fatty acids in human stool derivatized with (12)C- and (13)C-labelled aniline. J Pharm Biomed Anal 2017;138:43–53.

45. Engevik MA, Aihara E, Montrose MH, Shull GE, Hassett DJ, Worrell RT. Loss of NHE3 alters gut microbiota composition and influences Bacteroides thetaiotaomicron growth. Am J Physiol Gastrointest Liver Physiol 2013;305:G697–G711.

46. Chang-Graham AL, Danhof HA, Engevik MA, Tomaro-Duchesneau C, Karandikar UC, Estes MK, Versalovic J, Britton RA, Hyser JM. Human intestinal enteroids with inducible neurogenin-3 expression as a novel model of gut hormone secretion. Cell Mol Gastroenterol Hepatol 2019;8:209–229.

47. Engevik MA, Danhof HA, Chang-Graham AL, Spinler JK, Engevik KA, Herrmann B, Endres BT, Garey KW, Hyser JM, Britton RA, Versalovic J. Human intestinal enteroids as a model of Clostridioides difficile-induced enteritis. Am J Physiol Gastrointest Liver Physiol 2020; 318:G870–G888.

48. Ruan W, Engevik MA, Chang-Graham AL, Danhof HA, Goodwin A, Engevik KA, Shi Z, Hall A, Rienzi SCD, Venable S, Britton RA, Hyser J, Versalovic J. Enhancing

responsiveness of human jejunal enteroids to host and microbial stimuli. J Physiol 2020;598:3085–3105.

49. Saxena K, Blutt SE, Ettayebi K, Zeng XL, Broughman JR, Crawford SE, Karandikar UC, Sastri NP, Conner ME, Opekun AR, Graham DY, Qureshi W, Sherman V, Foulke-Abel J, In J, Kovbasnjuk O, Zachos NC, Donowitz M, Estes MK. Human intestinal enteroids: a new model to study human rotavirus infection, host restriction, and pathophysiology. J Virol 2016;90:43–56.

50. VanDussen KL, Marinshaw JM, Shaikh N, Miyoshi H, Moon C, Tarr PI, Ciorba MA, Stappenbeck TS. Development of an enhanced human gastrointestinal epithelial culture system to facilitate patient-based assays. Gut 2015;64:911–920.

51. Ettayebi K, Crawford SE, Murakami K, Broughman JR, Karandikar U, Tenge VR, Neill FH, Blutt SE, Zeng XL, Qu L, Kou B, Opekun AR, Burrin D, Graham DY, Ramani S, Atmar RL, Estes MK. Replication of human noroviruses in stem cell-derived human enteroids. Science 2016;353:1387–1393.

52. Foulke-Abel J, In J, Kovbasnjuk O, Zachos NC, Ettayebi K, Blutt SE, Hyser JM, Zeng XL, Crawford SE, Broughman JR, Estes MK, Donowitz M. Human enteroids as an ex-vivo model of host-pathogen interactions in the gastrointestinal tract. Exp Biol Med (Maywood) 2014;239:1124–1134.

53. Foulke-Abel J, In J, Yin J, Zachos NC, Kovbasnjuk O, Estes MK, de Jonge H, Donowitz M. Human enteroids as a model of upper small intestinal ion transport physiology and pathophysiology. Gastroenterology 2016; 150:638–649 e8.

54. Saxena K, Simon LM, Zeng XL, Blutt SE, Crawford SE, Sastri NP, Karandikar UC, Ajami NJ, Zachos NC, Kovbasnjuk O, Donowitz M, Conner ME, Shaw CA, Estes MK. A paradox of transcriptional and functional innate interferon responses of human intestinal enteroids to enteric virus infection. Proc Natl Acad Sci U S A 2017; 114:E570–E579.

55. Zachos NC, Kovbasnjuk O, Foulke-Abel J, In J, Blutt SE, de Jonge HR, Estes MK, Donowitz M. Human enteroids/colonoids and intestinal organoids functionally recapitulate normal intestinal physiology and pathophysiology. J Biol Chem 2016;291:3759–3766.

56. Zou WY, Blutt SE, Crawford SE, Ettayebi K, Zeng XL, Saxena K, Ramani S, Karandikar UC, Zachos NC, Estes MK. Human intestinal enteroids: new models to study gastrointestinal virus infections. Methods Mol Biol 2019;1576:229–247.

57. Endres B, Basseres E, Rashid T, Chang L, Alam MJ, Garey KW. A protocol to characterize the morphological changes of Clostridium difficile in response to antibiotic treatment. J Vis Exp 2017;123:55383.

58. Langendijk PS, Schut F, Jansen GJ, Raangs GC, Kamphuis GR, Wilkinson MH, Welling GW. Quantitative fluorescence in situ hybridization of Bifidobacterium spp. with genus-specific 16S rRNA-targeted probes and its application in fecal samples. Appl Environ Microbiol 1995;61:3069–3075.

59. Engevik MA, Engevik KA, Yacyshyn MB, Wang J, Hassett DJ, Darien B, Yacyshyn BR, Worrell RT. Human Clostridium difficile infection: inhibition of NHE3 and microbiota profile. Am J Physiol Gastrointest Liver Physiol 2015;308:G497–G509.

60. Engevik MA, Yacyshyn MB, Engevik KA, Wang J, Darien B, Hassett DJ, Yacyshyn BR, Worrell RT. Human Clostridium difficile infection: altered mucus production and composition. Am J Physiol Gastrointest Liver Physiol 2015;308:G510–G524.

61. Wang YM, Ge XZ, Wang WQ, Wang T, Cao HL, Wang BL, Wang BM. Lactobacillus rhamnosus GG supernatant upregulates serotonin transporter expression in intestinal epithelial cells and mice intestinal tissues. Neurogastroenterol Motil 2015;27:1239–1248.

62. Franich NR, Fitzsimons HL, Fong DM, Klugmann M, During MJ, Young D. AAV vector-mediated RNAi of mutant huntingtin expression is neuroprotective in a novel genetic rat model of Huntington's disease. Mol Ther 2008;16:947–956.

63. Miyamoto Y, Watanabe K, Tanaka R, Itoh K. Distribution analysis of six predominant Bacteroides species in normal human feces using 16S rDNA-targeted species-specific primers. Microbial Ecol Health Dis 2002; 14:133–136.

64. Li Z, Chalazonitis A, Huang YY, Mann JJ, Margolis KG, Yang QM, Kim DO, Cote F, Mallet J, Gershon MD. Essential roles of enteric neuronal serotonin in gastrointestinal motility and the development/survival of enteric dopaminergic neurons. J Neurosci 2011;31:8998–9009.

65. Carson JP, Eichele G, Chiu W. A method for automated detection of gene expression required for the establishment of a digital transcriptome-wide gene expression atlas. J Microsc 2005;217:275–281.

66. Hsiao EY, McBride SW, Hsien S, Sharon G, Hyde ER, McCue T, Codelli JA, Chow J, Reisman SE, Petrosino JF, Patterson PH, Mazmanian SK. Microbiota modulate behavioral and physiological abnormalities associated with neurodevelopmental disorders. Cell 2013;155:1451–1463.

67. Deacon RM. Digging and marble burying in mice: simple methods for in vivo identification of biological impacts. Nat Protoc 2006;1:122–124.

68. Angoa-Perez M, Kane MJ, Briggs DI, Francescutti DM, Kuhn DM. Marble burying and nestlet shredding as tests of repetitive, compulsive-like behaviors in mice. J Vis Exp 2013;82:50978.

69. Wertman V, Gromova A, La Spada AR, Cortes CJ. Low-cost gait analysis for behavioral phenotyping of mouse models of neuromuscular disease. J Vis Exp 2019;149.

70. Heck DH, Zhao Y, Roy S, LeDoux MS, Reiter LT. Analysis of cerebellar function in Ube3a-deficient mice reveals novel genotype-specific behaviors. Hum Mol Genet 2008;17:2181–2189.

71. Stanley JL, Lincoln RJ, Brown TA, McDonald LM, Dawson GR, Reynolds DS. The mouse beam walking assay offers improved sensitivity over the mouse rotarod in determining motor coordination deficits induced by benzodiazepines. J Psychopharmacol 2005;19:221–227.

72. Ventura M, Turroni F, Zomer A, Foroni E, Giubellini V, Bottacini F, Canchaya C, Claesson MJ, He F, Mantzourani M, Mulas L, Ferrarini A, Gao B,

Delledonne M, Henrissat B, Coutinho P, Oggioni M, Gupta RS, Zhang Z, Beighton D, Fitzgerald GF, O'Toole PW, van Sinderen D. The Bifidobacterium dentium Bd1 genome sequence reflects its genetic adaptation to the human oral cavity. PLoS Genet 2009;5: e1000785.

73. Bellono NW, Bayrer JR, Leitch DB, Castro J, Zhang C, O'Donnell TA, Brierley SM, Ingraham HA, Julius D. Enterochromaffin cells are gut chemosensors that couple to sensory neural pathways. Cell 2017; 170:185–198 e16.

74. Bertrand PP, Bertrand RL. Serotonin release and uptake in the gastrointestinal tract. Auton Neurosci 2010; 153:47–57.

75. Linan-Rico A, Ochoa-Cortes F, Beyder A, Soghomonyan S, Zuleta-Alarcon A, Coppola V, Christofi FL. Mechanosensory signaling in enterochromaffin cells and 5-HT release: potential implications for gut inflammation. Front Neurosci 2016;10:564.

76. Lund ML, Egerod KL, Engelstoft MS, Dmytriyeva O, Theodorsson E, Patel BA, Schwartz TW. Enterochromaffin 5-HT cells - a major target for GLP-1 and gut microbial metabolites. Mol Metab 2018;11:70–83.

77. Kushnir-Sukhov NM, Brown JM, Wu Y, Kirshenbaum A, Metcalfe DD. Human mast cells are capable of serotonin synthesis and release. J Allergy Clin Immunol 2007; 119:498–499.

78. Ringvall M, Ronnberg E, Wernersson S, Duelli A, Henningsson F, Abrink M, Garcia-Faroldi G, Fajardo I, Pejler G. Serotonin and histamine storage in mast cell secretory granules is dependent on serglycin proteoglycan. J Allergy Clin Immunol 2008;121:1020–1026.

79. Cote F, Thevenot E, Fligny C, Fromes Y, Darmon M, Ripoche MA, Bayard E, Hanoun N, Saurini F, Lechat P, Dandolo L, Hamon M, Mallet J, Vodjdani G. Disruption of the nonneuronal tph1 gene demonstrates the importance of peripheral serotonin in cardiac function. Proc Natl Acad Sci U S A 2003;100:13525–13530.

80. Walther DJ, Peter JU, Bashammakh S, Hortnagl H, Voits M, Fink H, Bader M. Synthesis of serotonin by a second tryptophan hydroxylase isoform. Science 2003; 299:76.

81. Khailova L, Mount Patrick SK, Arganbright KM, Halpern MD, Kinouchi T, Dvorak B. Bifidobacterium bifidum reduces apoptosis in the intestinal epithelium in necrotizing enterocolitis. Am J Physiol Gastrointest Liver Physiol 2010;299:G1118–G1127.

82. Hughes KR, Harnisch LC, Alcon-Giner C, Mitra S, Wright CJ, Ketskemety J, van Sinderen D, Watson AJ, Hall LJ. Bifidobacterium breve reduces apoptotic epithelial cell shedding in an exopolysaccharide and MyD88-dependent manner. Open Biol 2017;7:160155.

83. Apelqvist A, Li H, Sommer L, Beatus P, Anderson DJ, Honjo T, Hrabe de Angelis M, Lendahl U, Edlund H. Notch signalling controls pancreatic cell differentiation. Nature 1999;400:877–881.

84. Gradwohl G, Dierich A, LeMeur M, Guillemot F. Neurogenin3 is required for the development of the four endocrine cell lineages of the pancreas. Proc Natl Acad Sci U S A 2000;97:1607–1611.

85. Jenny M, Uhl C, Roche C, Duluc I, Guillermin V, Guillemot F, Jensen J, Kedinger M, Gradwohl G. Neurogenin3 is differentially required for endocrine cell fate specification in the intestinal and gastric epithelium. EMBO J 2002;21:6338–6347.

86. Jensen J, Heller RS, Funder-Nielsen T, Pedersen EE, Lindsell C, Weinmaster G, Madsen OD, Serup P. Independent development of pancreatic alpha- and beta-cells from neurogenin3-expressing precursors: a role for the notch pathway in repression of premature differentiation. Diabetes 2000;49:163–176.

87. Neufeld KM, Kang N, Bienenstock J, Foster JA. Reduced anxiety-like behavior and central neurochemical change in germ-free mice. Neurogastroenterol Motil 2011; 23:255–264, e119.

88. Nishino R, Mikami K, Takahashi H, Tomonaga S, Furuse M, Hiramoto T, Aiba Y, Koga Y, Sudo N. Commensal microbiota modulate murine behaviors in a strictly contamination-free environment confirmed by culture-based methods. Neurogastroenterol Motil 2013; 25:521–528.

89. Neufeld KA, Kang N, Bienenstock J, Foster JA. Effects of intestinal microbiota on anxiety-like behavior. Commun Integr Biol 2011;4:492–494.

90. Desbonnet L, Clarke G, Shanahan F, Dinan TG, Cryan JF. Microbiota is essential for social development in the mouse. Mol Psychiatry 2014;19:146–148.

91. Honda S, Kawaura K, Soeda F, Shirasaki T, Takahama K. The potent inhibitory effect of tipepidine on marble-burying behavior in mice. Behav Brain Res 2011; 216:308–312.

92. Broekkamp CL, Rijk HW, Joly-Gelouin D, Lloyd KL. Major tranquillizers can be distinguished from minor tranquillizers on the basis of effects on marble burying and swim-induced grooming in mice. Eur J Pharmacol 1986;126:223–229.

93. Ichimaru Y, Egawa T, Sawa A. 5-HT1A-receptor subtype mediates the effect of fluvoxamine, a selective serotonin reuptake inhibitor, on marble-burying behavior in mice. Jpn J Pharmacol 1995;68:65–70.

94. Takeuchi H, Yatsugi S, Yamaguchi T. Effect of YM992, a novel antidepressant with selective serotonin re-uptake inhibitory and 5-HT 2A receptor antagonistic activity, on a marble-burying behavior test as an obsessive-compulsive disorder model. Jpn J Pharmacol 2002; 90:197–200.

95. Li X, Morrow D, Witkin JM. Decreases in nestlet shredding of mice by serotonin uptake inhibitors: comparison with marble burying. Life Sci 2006;78:1933–1939.

96. Nicolas LB, Kolb Y, Prinssen EP. A combined marble burying-locomotor activity test in mice: a practical screening test with sensitivity to different classes of anxiolytics and antidepressants. Eur J Pharmacol 2006; 547:106–115.

97. Kim M, Cooke HJ, Javed NH, Carey HV, Christofi F, Raybould HE. D-glucose releases 5-hydroxytryptamine from human BON cells as a model of enterochromaffin cells. Gastroenterology 2001;121:1400–1406.

98. Haugen M, Dammen R, Svejda B, Gustafsson BI, Pfragner R, Modlin I, Kidd M. Differential signal pathway

activation and 5-HT function: the role of gut entero-chromaffin cells as oxygen sensors. Am J Physiol Gastrointest Liver Physiol 2012;303:G1164–G1173.

99. Zelkas L, Raghupathi R, Lumsden AL, Martin AM, Sun E, Spencer NJ, Young RL, Keating DJ. Serotonin-secreting enteroendocrine cells respond via diverse mechanisms to acute and chronic changes in glucose availability. Nutr Metab (Lond) 2015;12:55.

100. Essand M, Vikman S, Grawe J, Gedda L, Hellberg C, Oberg K, Totterman TH, Giandomenico V. Identification and characterization of a novel splicing variant of vesicular monoamine transporter 1. J Mol Endocrinol 2005; 35:489–501.

101. Nozawa K, Kawabata-Shoda E, Doihara H, Kojima R, Okada H, Mochizuki S, Sano Y, Inamura K, Matsushime H, Koizumi T, Yokoyama T, Ito H. TRPA1 regulates gastrointestinal motility through serotonin release from enterochromaffin cells. Proc Natl Acad Sci U S A 2009;106:3408–3413.

102. Schafermeyer A, Gratzl M, Rad R, Dossumbekova A, Sachs G, Prinz C. Isolation and receptor profiling of ileal enterochromaffin cells. Acta Physiol Scand 2004; 182:53–62.

103. Fukumoto S, Tatewaki M, Yamada T, Fujimiya M, Mantyh C, Voss M, Eubanks S, Harris M, Pappas TN, Takahashi T. Short-chain fatty acids stimulate colonic transit via intraluminal 5-HT release in rats. Am J Physiol Regul Integr Comp Physiol 2003;284:R1269–R1276.

104. Esmaili A, Nazir SF, Borthakur A, Yu D, Turner JR, Saksena S, Singla A, Hecht GA, Alrefai WA, Gill RK. Enteropathogenic Escherichia coli infection inhibits intestinal serotonin transporter function and expression. Gastroenterology 2009;137:2074–2083.

105. Nzakizwanayo J, Dedi C, Standen G, Macfarlane WM, Patel BA, Jones BV. Escherichia coli Nissle 1917 enhances bioavailability of serotonin in gut tissues through modulation of synthesis and clearance. Sci Rep 2015; 5:17324.

106. Bogunovic M, Dave SH, Tilstra JS, Chang DT, Harpaz N, Xiong H, Mayer LF, Plevy SE. Enteroendocrine cells express functional Toll-like receptors. Am J Physiol Gastrointest Liver Physiol 2007;292:G1770–G1783.

107. Nakaita Y, Kaneda H, Shigyo T. Heat-killed Lactobacillus brevis SBC8803 induces serotonin release from intestinal cells. Food Nutr Sci 2013;4:767–771.

108. Roy D, Ward P. Rapid detection of Bifidobacterium dentium by enzymatic hydrolysis of β-glucuronide substrates. J Food Protect 1992;55:291–295.

109. Fujimiya M, Okumiya K, Kuwahara A. Immunoelectron microscopic study of the luminal release of serotonin from rat enterochromaffin cells induced by high intraluminal pressure. Histochem Cell Biol 1997;108:105–113.

110. Patel BA, Bian X, Quaiserova-Mocko V, Galligan JJ, Swain GM. In vitro continuous amperometric monitoring of 5-hydroxytryptamine release from enterochromaffin cells of the guinea pig ileum. Analyst 2007;132:41–47.

111. Bertrand PP, Hu X, Mach J, Bertrand RL. Serotonin (5-HT) release and uptake measured by real-time electrochemical techniques in the rat ileum. Am J Physiol Gastrointest Liver Physiol 2008;295:G1228–G1236.

112. Ahlman H, Bhargava HN, Dahlstrom A, Larsson I, Newson B, Pettersson G. On the presence of serotonin in the gut lumen and possible release mechanisms. Acta Physiol Scand 1981;112:263–269.

113. Forsberg EJ, Miller RJ. Cholinergic agonists induce vectorial release of serotonin from duodenal enterochromaffin cells. Science 1982;217:355–356.

114. Fujimiya M, Yamamoto H, Kuwahara A. Effect of VIP and PACAP on vascular and luminal release of serotonin from isolated perfused rat duodenum. Ann N Y Acad Sci 1998;865:495–502.

115. Tsukamoto K, Ariga H, Mantyh C, Pappas TN, Yanagi H, Yamamura T, Takahashi T. Luminally released serotonin stimulates colonic motility and accelerates colonic transit in rats. Am J Physiol Regul Integr Comp Physiol 2007;293:R64–R69.

116. Oleskin AV, Kirovskaia TA, Botvinko IV, Lysak LV. [Effect of serotonin (5-hydroxytryptamine) on the growth and differentiation of microorganisms]. Mikrobiologiia 1998; 67:305–312.

117. Tsavkelova EA, Klimova S, Cherdyntseva TA, Netrusov AI. [Hormones and hormone-like substances of microorganisms: a review]. Prikl Biokhim Mikrobiol 2006; 42:261–268.

118. Knecht LD, O'Connor G, Mittal R, Liu XZ, Daftarian P, Deo SK, Daunert S. Serotonin activates bacterial quorum sensing and enhances the virulence of Pseudomonas aeruginosa in the host. EBioMedicine 2016;9:161–169.

119. Rios-Covian D, Gueimonde M, Duncan SH, Flint HJ, de los Reyes-Gavilan CG. Enhanced butyrate formation by cross-feeding between Faecalibacterium prausnitzii and Bifidobacterium adolescentis. FEMS Microbiol Lett 2015;362:fnv176.

120. Turroni F, Milani C, Duranti S, Mahony J, van Sinderen D, Ventura M. Glycan utilization and cross-feeding activities by Bifidobacteria. Trends Microbiol 2018;26:339–350.

121. Spencer NJ, Nicholas SJ, Robinson L, Kyloh M, Flack N, Brookes SJ, Zagorodnyuk VP, Keating DJ. Mechanisms underlying distension-evoked peristalsis in guinea pig distal colon: is there a role for enterochromaffin cells? Am J Physiol Gastrointest Liver Physiol 2011; 301:G519–G527.

122. Heredia DJ, Gershon MD, Koh SD, Corrigan RD, Okamoto T, Smith TK. Important role of mucosal serotonin in colonic propulsion and peristaltic reflexes: in vitro analyses in mice lacking tryptophan hydroxylase 1. J Physiol 2013;591:5939–5957.

123. Bercik P, Park AJ, Sinclair D, Khoshdel A, Lu J, Huang X, Deng Y, Blennerhassett PA, Fahnestock M, Moine D, Berger B, Huizinga JD, Kunze W, McLean PG, Bergonzelli GE, Collins SM, Verdu EF. The anxiolytic effect of Bifidobacterium longum NCC3001 involves vagal pathways for gut-brain communication. Neurogastroenterol Motil 2011;23:1132–1139.

124. Messaoudi M, Lalonde R, Violle N, Javelot H, Desor D, Nejdi A, Bisson JF, Rougeot C, Pichelin M, Cazaubiel M, Cazaubiel JM. Assessment of psychotropic-like properties of a probiotic formulation (Lactobacillus helveticus R0052 and Bifidobacterium longum R0175) in rats and human subjects. Br J Nutr 2011;105:755–764.

125. Desbonnet L, Garrett L, Clarke G, Kiely B, Cryan JF, Dinan TG. Effects of the probiotic Bifidobacterium infantis in the maternal separation model of depression. Neuroscience 2010;170:1179–1188.

126. Pinto-Sanchez MI, Hall GB, Ghajar K, Nardelli A, Bolino C, Lau JT, Martin FP, Cominetti O, Welsh C, Rieder A, Traynor J, Gregory C, De Palma G, Pigrau M, Ford AC, Macri J, Berger B, Bergonzelli G, Surette MG, Collins SM, Moayyedi P, Bercik P. Probiotic Bifidobacterium longum NCC3001 reduces depression scores and alters brain activity: a pilot study in patients with irritable bowel syndrome. Gastroenterology 2017; 153:448–459 e8.

127. Luck B, Engevik MA, Ganesh BP, Lackey EP, Lin T, Balderas M, Major A, Runge J, Luna RA, Sillitoe RV, Versalovic J. Bifidobacteria shape host neural circuits during postnatal development by promoting synapse formation and microglial function. Sci Rep 2020;10:7737.

128. Sachs BD, Rodriguiz RM, Siesser WB, Kenan A, Royer EL, Jacobsen JP, Wetsel WC, Caron MG. The effects of brain serotonin deficiency on behavioural disinhibition and anxiety-like behaviour following mild early life stress. Int J Neuropsychopharmacol 2013;16:2081–2094.

129. Fossat P, Bacque-Cazenave J, De Deurwaerdere P, Cattaert D, Delbecque JP. Serotonin, but not dopamine, controls the stress response and anxiety-like behavior in the crayfish Procambarus clarkii. J Exp Biol 2015; 218:2745–2752.

130. Fossat P, Bacque-Cazenave J, De Deurwaerdere P, Delbecque JP, Cattaert D. Comparative behavior. Anxiety-like behavior in crayfish is controlled by serotonin. Science 2014;344:1293–1297.

131. Heisler LK, Zhou L, Bajwa P, Hsu J, Tecott LH. Serotonin 5-HT(2C) receptors regulate anxiety-like behavior. Genes Brain Behav 2007;6:491–496.

132. Xiang M, Jiang Y, Hu Z, Yang Y, Botchway BOA, Fang M. Stimulation of anxiety-like behavior via ERK pathway by competitive serotonin receptors 2A and 1A in post-traumatic stress disordered mice. Neurosignals 2017;25:39–53.

133. Holmes A, Lit Q, Murphy DL, Gold E, Crawley JN. Abnormal anxiety-related behavior in serotonin transporter null mutant mice: the influence of genetic background. Genes Brain Behav 2003;2:365–380.

134. Sudo N, Chida Y, Aiba Y, Sonoda J, Oyama N, Yu XN, Kubo C, Koga Y. Postnatal microbial colonization programs the hypothalamic-pituitary-adrenal system for stress response in mice. J Physiol 2004;558:263–275.

135. Ramamoorthy S, Cool DR, Mahesh VB, Leibach FH, Melikian HE, Blakely RD, Ganapathy V. Regulation of the human serotonin transporter. Cholera toxin-induced stimulation of serotonin uptake in human placental choriocarcinoma cells is accompanied by increased serotonin transporter mRNA levels and serotonin transporter-specific ligand binding. J Biol Chem 1993; 268:21626–21631.

136. Guiard BP, Di Giovanni G. Central serotonin-2A (5-HT2A) receptor dysfunction in depression and epilepsy: the missing link? Front Pharmacol 2015;6:46.

137. Weisstaub NV, Zhou M, Lira A, Lambe E, Gonzalez-Maeso J, Hornung JP, Sibille E, Underwood M, Itohara S, Dauer WT, Ansorge MS, Morelli E, Mann JJ, Toth M, Aghajanian G, Sealfon SC, Hen R, Gingrich JA. Cortical 5-HT2A receptor signaling modulates anxiety-like behaviors in mice. Science 2006;313:536–540.

138. Lee JY, Jeon BS, Kim HJ, Park SS. Genetic variant of HTR2A associates with risk of impulse control and repetitive behaviors in Parkinson's disease. Parkinsonism Relat Disord 2012;18:76–78.

139. Borovikova LV, Ivanova S, Zhang M, Yang H, Botchkina GI, Watkins LR, Wang H, Abumrad N, Eaton JW, Tracey KJ. Vagus nerve stimulation attenuates the systemic inflammatory response to endotoxin. Nature 2000;405:458–462.

140. Wang X, Wang BR, Zhang XJ, Xu Z, Ding YQ, Ju G. Evidences for vagus nerve in maintenance of immune balance and transmission of immune information from gut to brain in STM-infected rats. World J Gastroenterol 2002;8:540–545.

141. Bercik P, Denou E, Collins J, Jackson W, Lu J, Jury J, Deng Y, Blennerhassett P, Macri J, McCoy KD, Verdu EF, Collins SM. The intestinal microbiota affect central levels of brain-derived neurotropic factor and behavior in mice. Gastroenterology 2011;141:599–609, e1-3.

142. Verdu EF, Bercik P, Verma-Gandhu M, Huang XX, Blennerhassett P, Jackson W, Mao Y, Wang L, Rochat F, Collins SM. Specific probiotic therapy attenuates antibiotic induced visceral hypersensitivity in mice. Gut 2006;55:182–190.

143. Carabotti M, Scirocco A, Maselli MA, Severi C. The gut-brain axis: interactions between enteric microbiota, central and enteric nervous systems. Ann Gastroenterol 2015;28:203–209.

144. Kunze WA, Mao YK, Wang B, Huizinga JD, Ma X, Forsythe P, Bienenstock J. Lactobacillus reuteri enhances excitability of colonic AH neurons by inhibiting calcium-dependent potassium channel opening. J Cell Mol Med 2009;13:2261–2270.

145. Iyer LM, Aravind L, Coon SL, Klein DC, Koonin EV. Evolution of cell-cell signaling in animals: did late horizontal gene transfer from bacteria have a role? Trends Genet 2004;20:292–299.

146. Arentsen T, Qian Y, Gkotzis S, Femenia T, Wang T, Udekwu K, Forssberg H, Diaz Heijtz R. The bacterial peptidoglycan-sensing molecule Pglyrp2 modulates brain development and behavior. Mol Psychiatry 2017; 22:257–266.

147. O'Mahony L, McCarthy J, Kelly P, Hurley G, Luo F, Chen K, O'Sullivan GC, Kiely B, Collins JK, Shanahan F, Quigley EM. Lactobacillus and bifidobacterium in irritable bowel syndrome: symptom responses and relationship to cytokine profiles. Gastroenterology 2005; 128:541–551.

148. Guglielmetti S, Mora D, Gschwender M, Popp K. Randomised clinical trial: Bifidobacterium bifidum MIMBb75 significantly alleviates irritable bowel syndrome and

improves quality of life–a double-blind, placebo-controlled study. Aliment Pharmacol Ther 2011;33:1123–1132.

149. O'Sullivan MA, O'Morain CA. Bacterial supplementation in the irritable bowel syndrome. A randomised double-blind placebo-controlled crossover study. Dig Liver Dis 2000;32:294–301.

150. Zocco MA, dal Verme LZ, Cremonini F, Piscaglia AC, Nista EC, Candelli M, Novi M, Rigante D, Cazzato IA, Ojetti V, Armuzzi A, Gasbarrini G, Gasbarrini A. Efficacy of Lactobacillus GG in maintaining remission of ulcerative colitis. Aliment Pharmacol Ther 2006;23:1567–1574.

151. Oliva S, Di Nardo G, Ferrari F, Mallardo S, Rossi P, Patrizi G, Cucchiara S, Stronati L. Randomised clinical trial: the effectiveness of Lactobacillus reuteri ATCC 55730 rectal enema in children with active distal ulcerative colitis. Aliment Pharmacol Ther 2012;35:327–334.

152. Kato K, Mizuno S, Umesaki Y, Ishii Y, Sugitani M, Imaoka A, Otsuka M, Hasunuma O, Kurihara R, Iwasaki A, Arakawa Y. Randomized placebo-controlled trial assessing the effect of Bifidobacteria-fermented milk on active ulcerative colitis. Aliment Pharmacol Ther 2004;20:1133–1141.